Journal of
Medicinal Chemistry

Article

De novo design of boron-based peptidomimetics as potent inhibitors of human ClpP in the presence of human ClpX

Joanne Tan, Julie G Grouleff, Yulia Jitkova, Diego B Diaz, Elizabeth Griffith, Wenjie Shao, Anastasia F. Bogdanchikova, Gennady Poda, Aaron D Schimmer, Richard E Lee, and Andrei K Yudin

J. Med. Chem., **Just Accepted Manuscript** • DOI: 10.1021/acs.jmedchem.9b00878 • Publication Date (Web): 12 Jun 2019

Just Accepted

is published by the American Chemical Society. 1155 Sixteenth Street N.W., Washington, DC 20036

De novo design of boron-based peptidomimetics as potent inhibitors of human ClpP in the presence of human ClpX

Joanne Tan[1], Julie J. Grouleff[2], Yulia Jitkova[3], Diego B. Diaz[1], Elizabeth C. Griffith[4], Wenjie Shao[1], Anastasia F. Bogdanchikova[1], Gennady Poda[2,5], Aaron D. Schimmer[3], Richard E. Lee[4] and Andrei K. Yudin[1*]

[1]Davenport Research Laboratories, Department of Chemistry, University of Toronto, 80 St. George Street, Toronto, ON, M5S 3H6, Canada, Email: ayudin@chem.utoronto.ca

[2]Drug Discovery Program, Ontario Institute for Cancer Research, MaRS Centre, 661 University Avenue, Suite 510, Toronto, ON, M5G 0A3, Canada

[3]Princess Margaret Cancer Centre, University Health Network, 610 University Avenue, Toronto, ON, M5G 2M9, Canada

[4]Department of Chemical Biology and Therapeutics, St. Jude Children's Research Hospital, 262 Danny Thomas Place, Memphis, TN, 38105-3678, USA

[5]Leslie Dan Faculty of Pharmacy, University of Toronto, 144 College Street, Toronto, ON, M5S 3M2, Canada

Abstract

Boronic acids have attracted the attention of synthetic and medicinal chemists due to boron's ability to modulate enzyme function. Recently, we demonstrated that boron-containing amphoteric building blocks facilitate the discovery of bioactive aminoboronic acids. Herein, we have augmented this capability with a *de novo* library design and virtural screening platform modified for covalent ligands. This technique has allowed us to rapidly design and identify a series of α-aminoboronic acids as the first inhibitors of human ClpXP, which is responsible for the degradation of misfolded proteins.

Introduction

Boron-containing molecules (BCMs) have garnered much attention over the years due to their recent successes as chemical probes and therapeutic agents.[1–7] The FDA approval of the multiple myeloma drug bortezomib[8] in 2008 led synthetic and medicinal chemists to reconsider the significance of boron in therapeutics. The empty *p* orbital of boronic acids can interact with nucleophilic amino acid residues forming a tetracoordinate "ate" complex. In addition, tricoordinate boron can adopt various coordination modes upon biological target engagement.[9] This stands in contrast to other electrophiles such as epoxides, aziridines, and Michael acceptors, which display a singular type of interaction with active site nucleophiles. Boron is also selective for oxygen nucleophiles, such as serine and threonine residues, which prevents cross-reactivity with cysteine residues.[10,11] Despite the versatility and recent successes of BCM-driven medicinal chemistry, there are still few examples of boron-containing therapeutic agents. This can be partially explained by the fact that synthetic technologies to site-selectively introduce boron into heteroatom-rich environments remain underdeveloped. The thermodynamic preference of boron to migrate from carbon to oxygen or nitrogen, further aggravated by the low kinetic barrier for these transformations, also accounts for the dearth of available methods.[12,13]

We recently developed a series of amphoteric molecules such as boryl aldehydes,[14,15] acyl boronates[16] and boryl isocyanides[17] and applied them for rapid construction of bioactive BCMs that contain numerous heteroatoms in the vicinity of boron. For instance, we have reported the synthesis of structurally novel boromorpholinone scaffolds from boryl isocyanides and demonstrated their role as potent inhibitors of the 20S proteasome.[17] We have also identified a novel β-aminoboronic acid chemotype as a cell-active inhibitor of the serine hydrolase, (ox)lipid-metabolizing enzyme α/β-hydrolyase domain 3 (ABHD3), where the *N*-methyliminodiacetic acid (MIDA) ligand increased the cellular permeability of the inhibitor.[18] To fully leverage the synthetic utility of boron-based amphoteric reagents, we now report on the integration of this chemistry with a *de novo* library design and virtual screening program and detail the discovery of bioactive inhibitors of human caseinolytic protease P.

Caseinolytic protease P (ClpP) is a highly conserved serine protease present in both bacteria and eukaryotes.[19,20] Its primary role is to maintain cellular homeostasis by working together with its AAA+ chaperones such as ClpA, ClpC and ClpX, to recognize, unfold, and translocate substrates into the proteolytic chamber of ClpP for protein degradation. In the absence of its chaperones, ClpP can only degrade small peptides. Thus far, research efforts in small molecule modulation of ClpP have been primarily directed towards bacteria.[19,21] This has led to the development of both activators and inhibitors of bacterial ClpP which can cause bactericidal inhibition, and impact bacterial virulence. Human ClpP (hClpP) is overexpressed in the mitochondria of a subset of acute myeloid leukemia (AML) cells and stem cells.[20] Therefore, inhibition or activation of hClpP has the potential to be an effective strategy for therapeutic intervention of AML.[21] In 2015, Sieber and coworkers identified phenyl ester AV167 as a low micromolar inhibitor of hClpP (IC_{50} = 1.54 μM).[22] More recently, Sieber has shown that TG42, an analogue of AV167, is a more potent and selective inhibitor of hClpP (IC_{50} = 0.39 μM) compared to AV167.[23] Additionally, TG42 was shown to inhibit the hClpP in the presence an acyldepsipeptide derived chaperone mimic and *Escherichia coli* ClpX (*Ec*ClpX) complex in a fluorescein-isothiocyanate-labelled casein

(FITC-casein) degradation assay and GFP degradation assay, respectively.[23] Despite inhibiting ClpP in the presence of its chaperone for the first time, the hClpP-*Ec*ClpX complex exhibits bacterial ClpXP substrate specificity which is more relevant for the development of antibiotics than as a therapeutic strategy for AML.[24] Currently, there are no selective, small molecule inhibitors of hClpP-hClpX complex which may be attributed to conformational changes in ClpP upon ClpX binding.[25,26]

In order to develop boron-containing inhibitors of hClpP, we opted to utilize a *de novo* design approach. Small molecule virtual screening has become a valuable tool in drug discovery. The benefit of this approach is that it negates the need to manually synthesize libraries of structurally diverse molecules, thus saving time and resources. For the docking of boronic acid-based ligands with hClpP, an important part of the screening process is to select only compounds which bind in a manner that allows for formation of a covalent bond between the boronic acid and the hydroxyl group of the catalytically active serine residue. A number of different software solutions exist for performing covalent docking,[27–30] however, none of them are optimally suited for screening a large user-designed library of covalent ligands, such as those synthesized using our amphoteric boron reagents. For many programs, only a small set of reactions can be performed, which limits their applicability. In addition, the side chain conformation of the reactive residue is often not optimized during the calculations, but instead treated as static, which means that the covalent docking results are heavily dependent on the chosen conformation of the residue. Furthermore, the majority of covalent docking methods are prohibitively slow when it comes to screening thousands of compounds. In 2014, the Shoichet lab developed the webserver DOCKovalent as a covalent docking program made for screening large libraries.[28] However, while it is well-suited for screening predetermined libraries of commercially available compounds, it cannot readily be used for screening user-designed libraries, and is thus not suitable for our chemistry. In light of these limitations of covalent docking programs, we developed a protocol for screening covalent inhibitors using a standard non-covalent docking method.

Herein, we show that chemistry derived from our boryl isocyanide building blocks combined with a *de novo* library design and virtual screening leads to peptidomimetic boron-based inhibitors of hClpP with low micromolar potency. The boron-based inhibitors are the first reported inhibitors of the more therapeutically relevant hClpXP protease.

Results and Discussion

Substrate-based hClpP inhibitor. The structures of the most celebrated boron-containing chemotherapeutics currently on the market are based on the α-aminoboronic acid motif. In fact, α-aminoboronic acids were shown to be selective inhibitors of *Mycobacterium tuberculosis* ClpP (*Mt*ClpP).[31,32] Therefore, we hypothesized that α-aminoboronic acids may also covalently inhibit the activity of hClpP. We synthesized compound **1**, which is an aminoboronic acid analogue of Phe-Ala-Pro-His-Phe (Figure 1). The boronic acid can interact with the catalytic serine (Ser97) upon binding to the active site. To synthesize boropeptide **1**, we first prepared benzyl-α-amino(MIDA)boronate. Starting from *N*-Cbz-benzyl-α-amino(MIDA)boronate, which was prepared according to literature procedures,[33] a hydrogenation with Pd/C was performed to obtain the benzyl-α-amino(MIDA)boronate. *N*-Ac-Phe-Ala-Pro-His-$B(OH)_2$ **1** was then prepared by coupling benzyl-α-amino(MIDA)boronate and the tetrapeptide *N*-Ac-Phe-Ala-Pro-His-OH (See Supporting Information, Scheme S1). Testing of **1** in a fluorescence-based Ac-Trp-Leu-Ala-AMC (WLA-AMC) assay confirmed that the compound is capable of inhibiting hClpP with an IC_{50} value of 27.27 ± 2.07 μM.

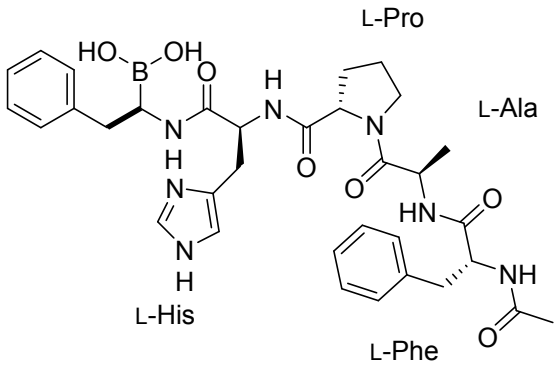

1

Figure 1: Boronic acid analoge of Phe-Ala-Pro-His-Phe.

Library enumeration. With the knowledge that α-aminoboronic acids display weak inhibitory activity towards hClpP, we realized that our amphoteric boron building blocks enabled us to synthesize peptidomimetic α-aminoboronic acids. Using our boryl isocyanide reagents, we performed an Ugi 4-component reaction (U4CR) with an aldehyde, amine and carboxylic acid.[17] The resulting compounds contain a similar molecular backbone to ClpP's natural peptide substrates. Based on the U4CR reaction, a four-component virtual library was enumerated using BIOVIA Pipeline Pilot[34] and the available chemical inventory in our laboratory: 89 aldehydes, 274 carboxylic acids and 8 boronic acid isocyanides were used (See Supporting Information for structures). The fourth component was kept constant as NH_3 in order to generate products that contain a secondary amide, which was shown to participate in hydrogen bonding to the carbonyl of Ser125 in ClpP's backbone. Among the aldehyde-containing building blocks, we kept only the ones with a single aldehyde group and no carboxylic acid functional groups. Likewise, among the carboxylic acid-containing building blocks, we kept only the ones with a single carboxylic acid and no aldehyde functional groups. The library enumeration resulted in 127,032 unique chemical structures. To eliminate reactive, chemically unstable at acidic conditions compounds and compounds with undesirable functional groups and unusual calculated physical properties, we applied a set of in-house High-Throughput Screening (HTS) Filters, developed in the Drug Discovery

group at Ontario Institute For Cancer Research as well as a set of lead-like filters based on calculated physical properties. Application of the filters reduced the virtual library size to 85,063 compounds. In order to determine which of these compounds would fit into the active site of hClpP, a virtual screen of the compound library was performed. As previously mentioned, none of the available covalent docking programs are well-suited for screening our custom library of α-aminoboronic acids. Therefore, we developed a new protocol for screening covalent inhibitors using a standard non-covalent docking method using Glide from Schrodinger, Inc.[35] The protocol involves three changes as compared to a regular virtual screening with Glide (Figure 2). For covalent ligands, it is essential that the docking procedure produces complexes where the reactive group on the ligand is in close proximity of the reactive residue in the target. However, complexes in which the reactive residue sidechain is as close to the ligand as it would be in a covalent complex will invariably lead to steric clashes, and thus an unfavorable docking score. To solve this, the reactive residue, Ser97, is mutated to a glycine prior to the docking calculation. Second, a distance constraint between the Cα atom of the reactive residue and the reactive group on the ligand is applied. This allows the reactive group in the ligand to be positioned in close contact with the reactive residue without the introduction of steric clashes. Lastly, for addition reactions, such as the reaction between a serine residue and a boronic acid, the geometry of the attachment atom on the ligand changes. In the case of a boronic acid addition, the boron changes from a trigonal to a tetrahedral geometry. To mimic this, an artificial conversion of each ligand is performed prior to the docking, which consists of adding a hydrogen atom to the boron atom. This allows the docking procedure to test whether the tetrahedral boronates that are formed upon interact with Ser97 will able to fit into the binding pocket. We specifically chose a hydrogen atom over an oxygen atom because an oxygen would be added in the form of a hydroxyl group (-OH) or hydroxide which is negatively charged. In combination, the three described deviations from a standard docking protocol; mutation of

reactive residue, distance constraint, and compound conversion, provide the basis for using a standard non-covalent docking program to screen covalent ligands.

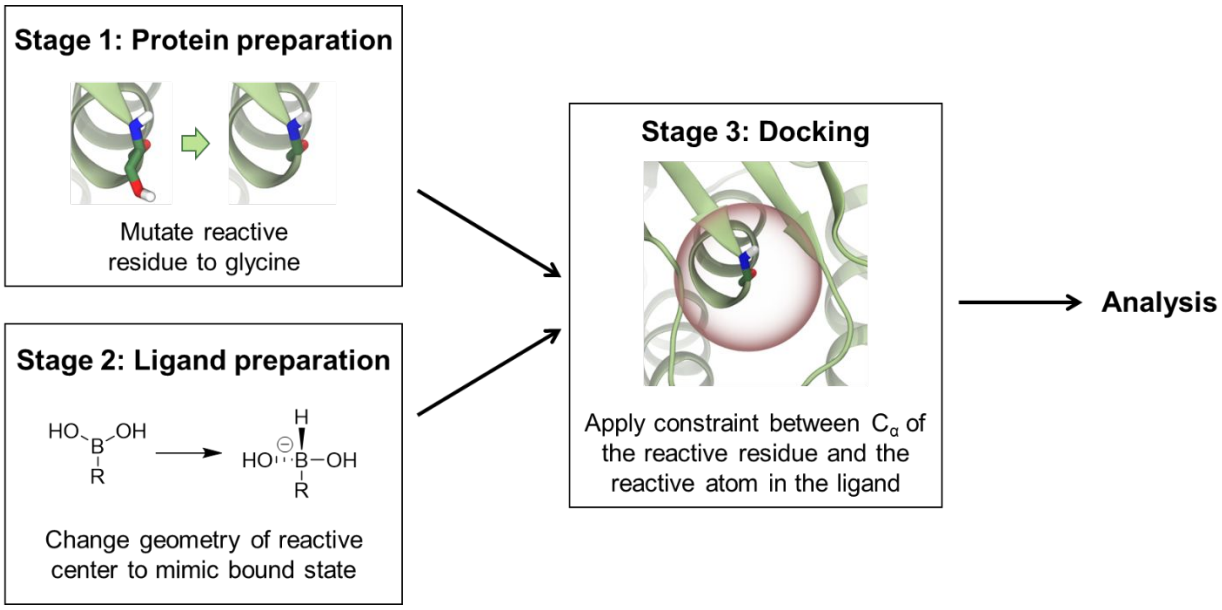

Figure 2: Depiction of the three changes made to a standard covalent docking protocol that makes it possible to use non-covalent docking to virtually screen large libraries of covalent ligands within a reasonable time.

The main caveat of this approach is that although the resulting poses will have the reacting atoms in the vicinity of each other, they will not necessarily be in an optimal position for covalent bond formation. Therefore, additional visual inspection of the results is needed for determining the most promising hits. Alternatively, geometric filters can be applied to the docking results, to only select poses that would allow the reactive residue to adopt a favorable conformer and at the same time keep the distance between the two reacting atoms close to the value of the equilibrium bond length for such an interaction. Ai *et al.* have also published a method for using non-covalent docking for screening covalent ligands, known as Steric-Clashes Alleviating Receptor (SCAR).[36] In SCAR, the reactive residue is also mutated to glycine, however there is no distance constraint between the reactive groups, and the geometry of the ligands is not changed prior to the docking calculation. Instead, the docking poses are tested after the calculation and only ligands

which have the two reactive groups in close vicinity are selected. This means that if the top-scoring poses of a given ligand does not fulfill the distance criteria it is discarding even though it might also be able to adopt a slightly less favorable mode in which the two groups do come close together. In our approach, we avoid such issues, since the distance constraint is applied during the actual docking.

Virtual screening and compound selection. The method described above was used to screen the U4CR library against the active site of hClpP. The 1,000 top-ranked compounds based on Glide SP docking score were subjected to further analysis in order to select compounds for synthesis. Due to the combinatorial nature of the library, it is possible to separate the analysis into three parts, focusing at finding the most favorable groups at the either the R^1, R^2 or R^3 position (See Supporting Information, Figure S1). Thus, an analysis was performed to determine the substituents that appeared most frequently at each of the three positions. The results of this analysis, combined with a visual inspection of the top-scoring poses to ensure that bond formation to Ser97 was possible for the chosen R^1, R^2 and R^3 substituents, was used to select a final set of substitutents predicted to be favorable for each position (See Supporting Information, Figure S1). Based on the observed binding mode of the docked compounds, the R^1 group was expected to impact the hClpP potency the most, followed by the group at the R^3 position. For the R^1 position, aliphatic groups such as isobutyl and *n*-butyl appeared to be well suited for filling out the S1 pocket. Phenyl and benzyl groups were predicted to be less favorable at the R^1 position compared to aliphatic groups. However, a compound containing a benzylic group at R^1 was still selected for synthesis in order to validate this hypothesis. For the R^2 position, aliphatic and phenyl groups were selected. For the R^3 position, aromatic groups dominated the top-scoring compounds, including phenylic compounds and bicyclic ring systems. Overall, these results are consistent with Sieber's findings on hClpP specificity derived from a fluorogenic library screening.[37] The molecules that were selected from this virtual library for synthesis were chosen

based on this analysis as well as synthetic feasibility and structural diversity (See Supporting Information, Figure S2).

Synthesis of α-aminoboronic acids. Based on the *in silico* screening results and synthetic feasibility, 9 molecules were selected for synthesis (See Supporting Information, Figure S2). We began the synthesis by subjecting isobutyl- or benzyl-substituted boryl isocyanide **2a** and **2b**, respectively, to an U4CR with an aldehyde, carboxylic acid and ammonia in TFE (Scheme 1). From this reaction, we obtained a 1:1 diastereomeric mixture of the desired α-amino(MIDA)boronates **3** which could be separated by normal-phase column chromatography. The compounds that were below 95% purity as determined by ^{1}H NMR were purified again by reverse-phase column chromatography. Out of the 9 molecules selected for synthesis, we were only able to synthesize 6 of them using the U4CR. For more details on the substrate tolerance of the reaction, please see the Supporting Information.

MIDA-protected boronates are inactive as serine hydrolase inhibitors due to the tetracoordinate environment around boron. Thus, MIDA is typically released *in situ* under the assays conditions or as a separate synthetic step prior to assay submission. Although α-aminoboronic acids possess the ability to inhibit serine hydrolases, they are susceptible to degradation through a 1,2-boryl migration.[13] However, acylation at this nitrogen atom engages the lone pair in an amide bond which eliminates the decomposition pathway. Thus, α-amino(MIDA)boronates **3** should be stable upon MIDA hydrolysis. We began our experiments by attempting to hydrolyze MIDA under basic conditions.[18] We were pleased to see formation of free boronic acids **4**, however, we also saw evidence of boric acid. On the other hand, the hydrolysis went smoothly with acid to provide the free boronic acid in quantitative yields. It is important to mention that this deprotection only proceeded at reasonable rates in alcoholic solvents and when using other solvents, degradation was observed over time. Unfortunately, the second diastereomer of compound **4d** did not readily undergo MIDA hydrolysis due to poor solubility.

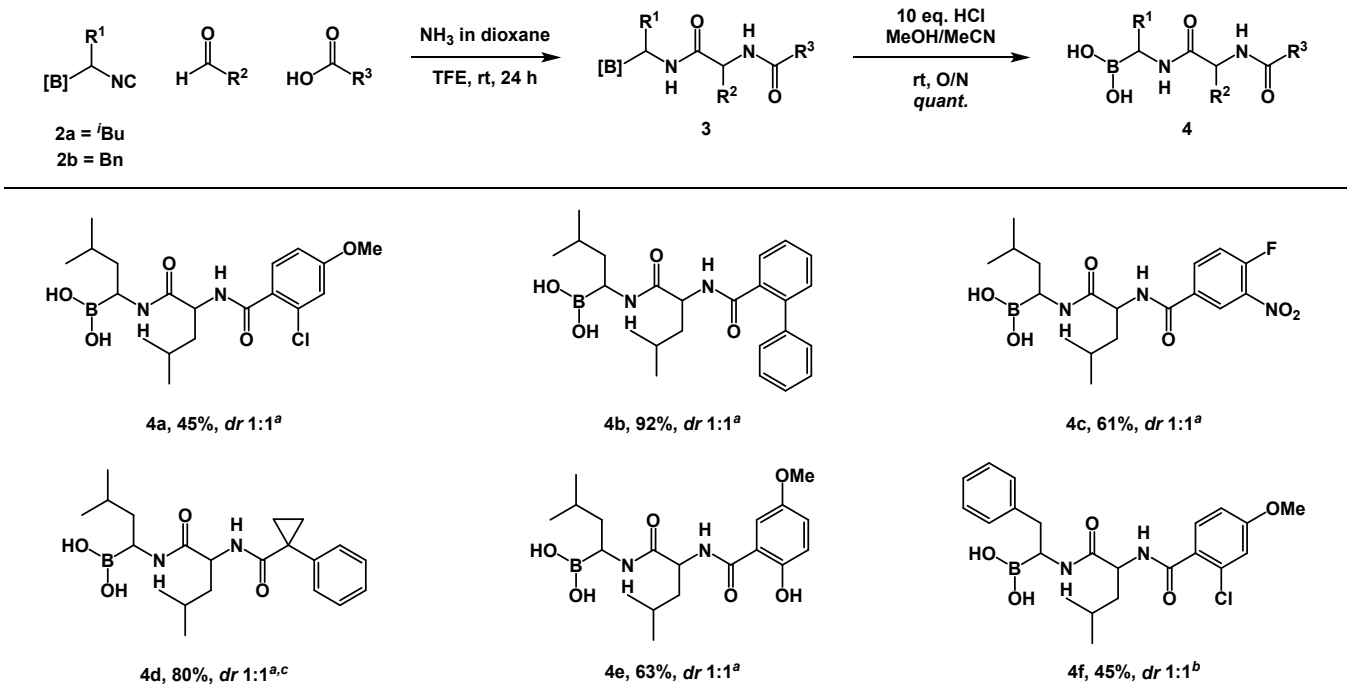

Scheme 1: Synthesis of α-aminoboronic acids from an U4CR reaction with our boryl isocyanide building blocks. [a]Synthesized from compound **2a**. [b]Synthesized from compound **2b**. [c]Unable to access the boronic acid through MIDA hydrolysis due to poor solubility of the starting material.

Initial testing for the inhibition of human ClpP. The racemic α-aminoboronic acids **4** were screened for hClpP inhibition in a fluorescence-based WLA-AMC assay in independent triplicates (Table 1). Ac-WLA-AMC has been recently reported as a substrate for human ClpP that is used for measuring its peptidase activity by monitoring release of fluorescent amino-methylcoumarin.[38] The *syn* and *anti* configurations of compounds **4** were assigned based on the relative positioning of the R^1 and R^2 side chains. The relative stereochemistry was assigned after a crystal structure of compound ***anti*-4a** bound to *Staphylococcus aureus* ClpP (*Sa*ClpP) was obtained as described in the next paragraph (Figure 3). Interestingly, only the second diastereomer ***anti*-4** of this series of compounds exhibited activity towards hClpP whereas the ***syn*-4** diastereomer was inactive. This suggests that stereochemistry plays an important role in binding. Compounds ***anti*-4a, *anti*-4b, *anti*-4c** and ***anti*-4e** displayed IC_{50} values of 41.9 ± 2.8, 18.4 ± 5.5, 28.9 ± 5.0 and 34.27 ± 7.84 μM, respectively. Compound ***anti*-4f**, which was synthesized to probe the P1 pocket

of hClpP, was significantly less potent than ***anti*-4a** (IC_{50} = 103.0 ± 31.1 μM). This result confirms that aliphatic groups are more favorable than benzylic groups at the R^1 position as predicted from the virtual screening results.

Table 1: IC_{50} values for the inhibition of hClpP by compounds **4** in WLA-AMC assay. The assay was performed in independent triplicates.

Compound Name	hClpP IC_{50} (μM)	
	***syn*-4** (Diastereomer 1)	***anti*-4** (Diastereomer 2)
4a	No inhibition	41.9 ± 2.8
4b	No inhibition	18.4 ± 5.5
4c	No inhibition	28.9 ± 5.0
4d	No inhibition	N/A[a]
4e	No inhibition	34.27 ± 7.84
4f	No inhibition	117.6 ± 1.01
AV167[b]	4.44 ± 0.18	

[a]Unable to synthesize boronic acid. [b]AV167 was tested as a positive control.

Crystal structure of ligand-bound bacterial ClpP. Crystallization trials to produce structural data depicting compound ***anti*-4a** bound to hClpP were undertaken but ultimately failed to produce data. *Sa*ClpP and hClpP display high protein sequence homology (See Supporting Information, Figure S3). As an alternative we utilized previously established *Sa*ClpP conditions to co-crystalize ***anti*-4a** with *Sa*ClpP to a resolution of 2.0 Å (PBD 6N80; See Supporting Information, Table S1). The structure displayed clear electron density for ***anti*-4a** confirming its binding mode (See Supporting Information, Figure S4). A comparison of the X-ray structure of ***anti*-4a** bound to *Sa*ClpP with the docking pose of ***anti*-4a** in hClpP from the non-covalent virtual screening reveals striking similarities (Figure 3). The predicted hydrogen bonds between the amide group in the compound and the backbone atoms in the protein are also observed in the X-ray structure. There is also excellent agreement between the predicted and observed interactions

of the boronic acid group with the protein. The main difference is observed at the R^3 position where the rotation angle of the phenyl ring differs by ~90°. This change is likely due to residue differences between the *Sa*ClpP and hClpP in this part of the binding site, including Thr146/Leu145 and His142/Glu141 (See Supporting Information, Figure S3, black). Overall, the similarity in binding mode for the docking pose and the X-ray structure show that our non-covalent protocol for docking covalent compounds is a valuable tool for predicting protein-ligand interactions and design of covalent inhibitors.

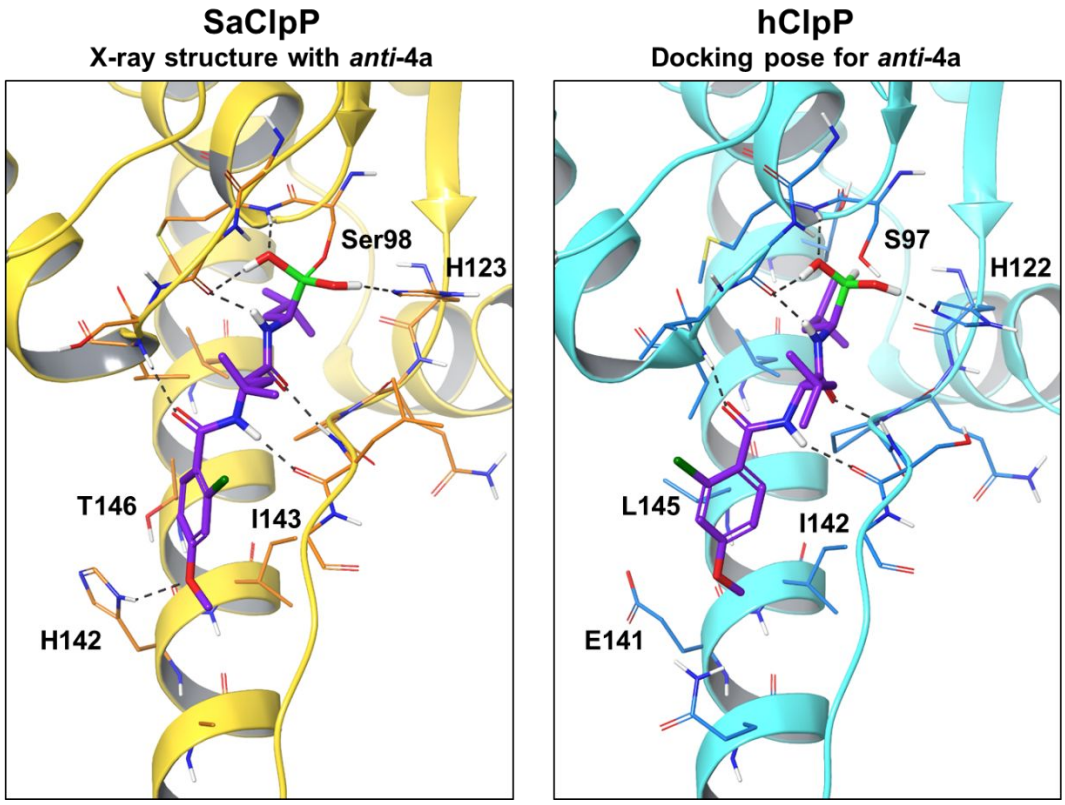

Figure 3: Binding modes of ***anti*-4a**. Left: X-ray structure of ***anti*-4a** (purple) bound to the active site of *Sa*ClpP (yellow, PDB:3STA). Right: Predicted binding mode of ***anti*-4a** (purple) in the active site of hClpP (blue, PDB: 1TG6). The compound was docked using the non-covalent docking protocol described in this paper. The dashed lines repesent hydrogen bonds between the ligand and the protein. The RMSD of SaClpP and hClpP protein backbone is 1.01 Å. The RMSD of heavy atoms between co-crystallized ***anti*-4a** with *Sa*ClpP and docked ***anti*-4a** with hClpP is 1.45 Å.

Synthesis of enantiomerically pure α-aminoboronates. Based on the results of the initial hClpP screening, compounds ***anti*-4a, *anti*-4b** and ***anti*-4c** were chosen for follow up studies. We decided to pursue the synthesis of the enantiopure variants given that is it likely we will see improvements in the potency. We began the synthesis with the protection of isobutyl boronic acid with (+)-pinanediol and (-)-pinanediol to afford (*S*)-pinanediol-2-methylpropane-1-boronate and (*R*)-pinanediol-2-methylpropane-1-boronate, respectively. Next, the Matteson homologation was performed using dichloromethane and *n*-butyllithium followed by zinc chloride addition to obtain the (*S*)-chloroboronate ester and (*R*)-chloroboronate ester in high diastereoselectivity (>95:5 based on HPLC of compounds **7**) from (*S*)-pinanediol-2-methylpropane-1-boronate and (*R*)-pinanediol-2-methylpropane-1-boronate, respectively.[39,40] The (*S*)-chloroboronate ester was then converted to the (*R*)-(*N*-TMS)$_2$-aminoboronate ester through an S_N2 reaction with LHMDS. Likewise, the (*R*)-chloroboronate ester was converted to the (*S*)-(*N*-TMS)$_2$-aminoboronate ester. The trimethylsilyl groups were removed using excess trifluoroacetic acid to provide (*R*)-aminoboronate ester **5a** and (*S*)-aminoboronate **5b** as the TFA salts (See Supporting Information, Scheme S2). At this point, we presumed there was no erosion of the enantiopurity and carried on to the next steps. The corresponding carboxylic acids **6** were prepared using standard Fmoc solid-phase synthesis with 2-chlorotrityl resin, HATU and DIPEA for the coupling, 30% piperidine in DMF for the Fmoc removal, and 25% HFIP in DCM for the resin cleavage (See Supporting Information for a list of carboxylic acids). Carboxylic acids **6a-c** were coupled to (*R*)-aminoboronate ester **5a** using TBTU and DIPEA in DCM to yield α-aminoboronates **7a-c** (Scheme 2). Carboxylic acid **6d** was coupled to (*S*)-aminoboronate ester **5b** using the same protocol to afford α-aminoboronate **7d** as the enantiomer of **7a**. The diastereoselectivity of α-aminoboronates **7** was analyzed by HPLC to be >95:5 which indicates there was no epimerization during the coupling step. Lastly, the α-aminoboronates **7a-d** were deprotected with 10 equivalents of aqueous HCl and phenylboronic acid for effective pinanediol transfer in hexanes:MeOH

(1:1) at room temperature to provide the α-aminoboronic acids **8a-d** in excellent yields.

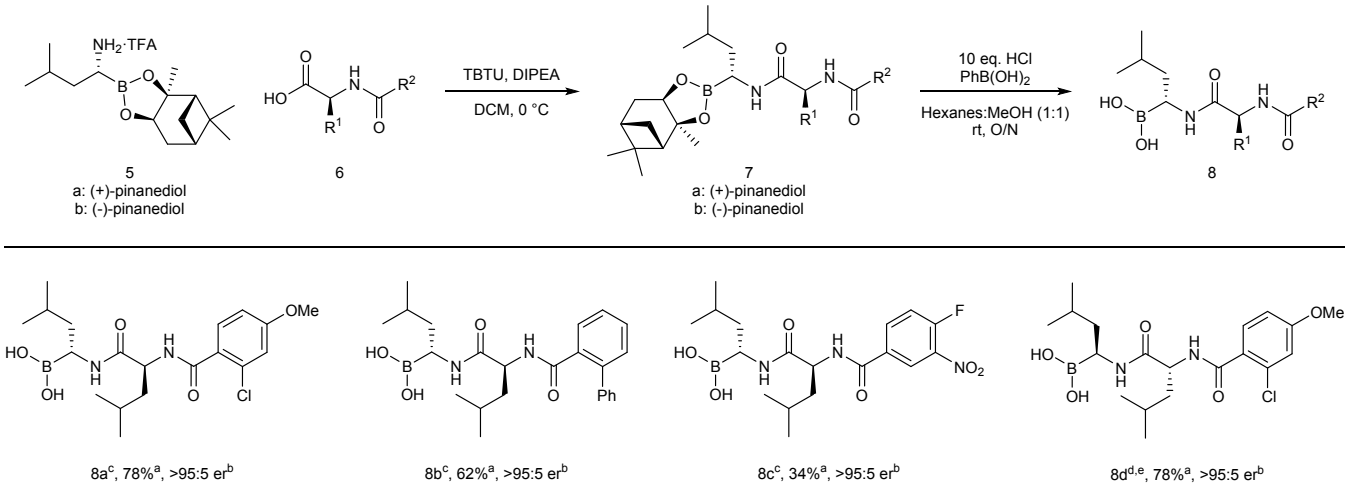

Scheme 2: Synthesis of enantiopure α-aminoboronates and boronic acids. [a]Yield is reported over two steps from **5**. [b]er is based on the dr of **7** from the HPLC trace. [c]Synthesized from **5a**. [d]Synthesized from **5b**. [e]Synthesized from **6d** containing D-leu.

Testing of enantiomerically pure α-aminoboronic acids for inhibition of human ClpP. With the enantiomerically pure α-aminoboronic acids **8** in hand, we began to screen them along with the corresponding racemate in the WLA-AMC assay. The IC_{50} values of compounds **8a**, **8b** and **8c** were 10.2 ± 3.7, 8.4 ± 2.6 and 12.4 ± 0.1 μM, respectively (Figure 4a). Therefore, the enantiomerically pure α-aminoboronic acids are up to four times more potent than the racemate. Compound **8d**, which is the enantiomer of **8a**, was unable to inhibit hClpP peptidase activity. This suggests that stereochemistry is important for binding to the hClpP active site.

Testing for inhibition of hClpP in the presence of hClpX. ClpXP performs protein degradation in cells[20] whereas ClpP can only degrade small peptides.[19] In 2015, Sieber and coworkers showed that AV167 was a potent inhibitor of hClpP; however, it was unable to inhibit hClpXP proteolysis.[22] More recently, TG42 was shown to inhibit the hClpP-*Ec*ClpX complex;[23] however, the hClpP-*Ec*ClpP complex displays

bacterial ClpXP substrate specificity and therefore, cannot degrade casein.[24,25] Thus, the development of selective, small molecule inihbitors of hClpP in the presence of hClpX is important in order to study the therapeutic relevance of hClpXP. We began by subjecting the enantiopure compounds **8a, 8b and 8c** and racemates ***anti*-4a, *anti*-4b** and ***anti*-4c** to a hClpXP FITC-casein assay in independent triplicates. ClpXP-induced proteolysis occurs through binding of a chaperone such as ClpX to the proteolytic component ClpP whereupon a functional ClpXP protease complex is formed. This assay is aimed at detecting the presence of protease activity of ClpXP by using casein labeled with fluorescein isothiocyanate as a substrate. The fluorescein label on the FITC-casein is highly quenched until it is digested into smaller peptides by ClpXP.[41] The IC_{50} values for inhibition of hClpXP protease activity of the enantiopure α-aminoboronic acids **8a**, **8b** and **8c** are 0.8 ± 0.3 μM , 0.9 ± 0.4 μM and 1.0 ± 0.3 μM, respectively (Figure 4b). These results indicate that α-aminoboronic acids are potent inhibitors of hClpXP and are unique in their ability to inhibit the holoenzyme.[26]

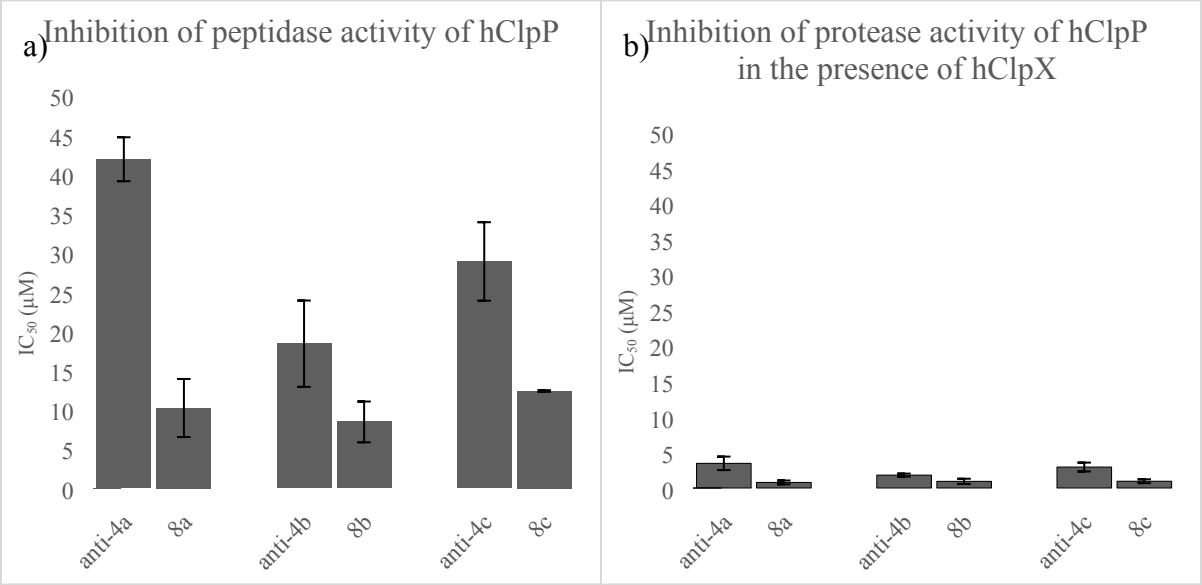

Figure 4: a) Inhibition of hClpP by racemic and enantiopure α-aminoboronic acids ***anti*-4** and **8**, respectively, in a WLA-AMC assay. The assay was performed in independent triplicates. b) Inhibition of hClpXP by racemic and enantiopure α-aminoboronic acids ***anti*-4** and **8**, respectively, in a FITC-casein assay. The assay was performed in independent triplicates.

Conclusions

For the first time, we have exemplified the power of combining our boron-based amphoteric reagents with a *de novo* library design and virtual screening in order to rapidly identify and generate bioactive boron-containing molecules for human ClpP and hClpP-hClpX complex. More specifically, we utilized our boryl isocyanides in a multicomponent Ugi reaction to synthesize peptidomimetic α-aminoboronic acids while the *de novo* virtual screening effectively analyzed and filtered all possible α-aminoboronic acid candidates. By integrating these two capabilities, we have successfully identified three α-aminoboronic acids as potent inhibitors of hClpP and hClpXP with IC_{50} values in the low micromolar range. These IC_{50} values were comparable to AV167 in our testing against hClpP but as opposed to AV167 and TG42, the α-aminoboronic acids also inhibited hClpXP. To the best of our knowledge, these α-aminoboronic acids are the first reported inhibitors of hClpXP. This work serves as a starting point for the development of more synthetically complex α-aminoboronic acid inhibitors of hClpXP.

Experimental Section

Chemistry. Synthesis. Methylene chloride (DCM), methanol (MeOH) and triethylamine were distilled from CaH_2 under nitrogen. Acetonitrile (MeCN) was distilled from activated 4Å MS under nitrogen. Tetrahydrofuran (THF) was freshly distilled from sodium benzophenone ketyl. Amino acid reagents were sourced from Chem-Impex International Inc. Peptide grade DIPEA was sourced from Sigma Aldrich. Peptide grade DMF were sourced from Caledon Laboratories Ltd. All other solvents were of reagent grade quality and dried over 4Å MS prior to use. All reagents were purchased from commercial sources and used as received. Flash column chromatography was carried out using Silicycle 230-400 mesh silica gel, or ISCO Teledyne Combiflash R_f 200 Flash system. Thin-layer chromatography (TLC) was performed on Macherey Nagel pre-coated glass backed TLC plates (SIL G/UV254, 0.25 mm) and visualized using a UV

lamp (254 nm), $KMnO_4$ or curcumin stain (preparation: 200 mg curcumin in 100 mL ethanol). Reverse-phase chromatography was carried out using Redi*Sep* Rf Gold C18 Columns. ^{1}H NMR, ^{13}C, and 2D NMR spectra were recorded on Varian Mercury 300 MHz, 400 MHz, 500 MHz, 600 MHz or 700 MHz spectrometers. ^{11}B NMR were recorded using Bruker 400/500 MHz spectrometer at 128/160 MHz and referenced to an external standard of $BF_3 \cdot Et_2O$ (δ = 0 ppm). ^{19}F NMR were recorded using Bruker 400 MHz spectrometer at 376 MHz and referenced to an external standard of $CFCl_3$ (δ = 0 ppm). ^{1}H NMR spectra chemical shifts (δ) are reported in parts per million (ppm) referenced to residual protonated solvent peak (CD_3CN δ = 1.94, DMSO-d_6, δ = 2.49, CD_3OD δ = 3.31, $CDCl_3$ δ = 7.26; center line). Spectral data is reported as follows: chemical shift, multiplicity (s = singlet, d = doublet, t = triplet, q = quartet, dd = doublet of doublets, dt = doublet of triplets, ddt = doublet of doublet of triplets, dtd = doublet of triplet of doublets, m = multiplet, br = broad), coupling constant (*J*) in Hertz (Hz), and integration. ^{13}C NMR spectra chemical shifts (δ) are reported in parts per million (ppm) were referenced to carbon resonances in the NMR solvent (CD_3CN δ = 118.3, DMSO-d_6, δ = 39.5, CD_3OD δ = 49.0, $CDCl_3$ δ = 77.2; center line). Carbons exhibiting significant line broadening brought about by boron substituents were not reported (quadrupolar relaxation). High resolution mass spectra were obtained on a VG 70- 250S (double focusing) mass spectrometer at 70 eV or on an ABI/Sciex Qstar mass spectrometer with ESI source, MS/MS and accurate mass capabilities. Low resolution mass spectra were obtained on an Agilent Technologies 1200 series HPLC paired to a 6130 Mass Spectrometer. Low-resolution mass spectra (ESI) were collected on an Agilent Technologies 1200 series HPLC paired to a 6130 Mass Spectrometer. Compounds were resolved on Phenomenex's Kinetex 2.6u C18 50x4.6mm column at room temperature with a flow of 1 mL/min. The gradient consisted of eluents A (0.1% formic acid in double distilled water) and B (0.1% formic acid in HPLC-grade acetonitrile). *Method A*: The flow rate was held at 1.0 mL/min. From 0 min to 4 min, was used a linear gradient starting from 5% of B to 95% of B. From 4 min to 5 min, the solvent was held at 95% of B. From 5 min to 5.5 min, was used a linear gradient from 95% of B to 5% of B. From

5.5 min to 6.5 min, the solvent was held at 5% of B. *Method B*: The flow rate was held at 1.5 ml/min. From 0 min to 15 min, was used a linear gradient starting from 5% of B to 95% of B. From 15 min to 19.5 min, the solvent was held at 95% of B. From 19.5 min to 20 min, the solvent was held at 5% of B. *Method C:* A linear gradient starting from 5% of B to 95% over 15 min at a flow rate of 1.0 mL/min. All compounds synthesized in this manuscript are >95% in purity unless otherwise stated. The purity was assessed using ^{1}H NMR and/or HPLC as listed above.

Synthesis of *N*-Ac-Phe-Ala-Pro-His(*N*-Trt)-Phe-B(OH)$_2$ (1). To a solution of *N*-Cbz-benzyl-α-amino(MIDA)boronate[33] (649 mg, 1.58 mmol, 1.0 equiv) in acetic acid (15 mL) was added palladium hydroxide 20% on carbon (111 mg, 0.158 mmol, 0.1 equiv). The reaction mixture was stirred at room temperature under an atmosphere of $H_{2(g)}$ for 3 h until the reaction was complete as indicated by LC-MS. The reaction mixture was filtered through a pad of Celite, rinsing with a total of 100 mL of acetonitrile. The filtrate was concentrated to dryness to afford the crude product as a yellowish solid in 87% yield (462 mg, 1.37 mmol). Benzyl-α-amino(MIDA)boronate was used in the next step without further purification. The *N*-acylated tetrapeptide [*N*-Ac-Phe-Ala-Pro-His(*N*-Trt)-OH] was assembled on 2-chlorotrityl chloride resin with manual loadings of each amino acid. The linear peptide was synthesized by conventional Fmoc solid phase-based peptide synthesis using single coupling steps with HATU in DIPEA. The peptide was cleaved from the resin by three successive washes, 0.5 h apart, with 1:4 HFIP/DCM. The cleavage layers were then evaporated and the tetrapeptide precipitated from diethyl ether. The tetrapeptide (102 mg, 0.135 mmol, 1.0 equiv) was added to a 2 Dram vial equipped with a magnetic stir and was dissolved in 2 mL of anhydrous DMF. In a separate vial, benzyl-α-amino(MIDA)boronate (56 mg, 0.167 mmol, 1.23 equiv) was stirred with Amberlite IRA743 free base in 1 mL of DMF for 20 minutes. The benzyl-α-amino(MIDA)boronate solution was then transferred via syringe to the vial containing the tetrapeptide. HATU (83.9 mg, 0.203 mmol, 1.5 equiv) and 2,6-lutidine (47 μL, 0.406 mmol, 3.0 equiv) were then added, and the reaction mixture was left to stir at room

temperature for 14 h. The reaction mixture was concentrated to about 1 mL of DMF and subsequently purified by C18 reverse-phase chromatography using a 0% → 75% acetonitrile gradient in water over 45 minutes. The fractions containing desired product were then lyophilized to afford the MIDA-protected boropeptide [*N*-Ac-Phe-Ala-Pro-His(*N*-Trt)-Phe-B(MIDA)] (51 mg, 50.3 μmol) in 37.2% yield as a white powder. NMR and LC-MS analysis confirmed that the MIDA-protected boropeptide was produced in a 1:1 mixture of diastereomers. The purity of *N*-Ac-Phe-Ala-Pro-His(*N*-Trt)-Phe-B(MIDA) was assessed by HPLC using Method A. Quantitative deprotection of the *N*-Trt-protected His side chain and the MIDA-group of *N*-Ac-Phe-Ala-Pro-His(*N*-Trt)-Phe-B(MIDA) was achieved using a solution of 3 M HCl (105 μL, 10 equiv) in 5:1 MeOH:H_2O (1 mL) solvent mixture with stirring for 12 h. The reaction mixture was then purified by C18 reverse-phase chromatography using a 0% → 50% acetonitrile gradient in water over 45 minutes. The fractions containing desired product were then lyophilized to afford *N*-Ac-Phe-Ala-Pro-His(*N*-Trt)-Phe-B$(OH)_2$ **1** (20.8 mg, 31.6 μmol) in quantitative yield as a white powder. The purity of **1** was assessed by HPLC using Method C.

Synthesis of boryl isocyanides (2). Boryl isocyanides were prepared using the following modified procedure.[17] To a flame-dried, two-neck round-bottom flask equipped with a magnetic stir bar under with nitrogen atmosphere, was added freshly distilled DCM (8 mL) which was cooled to 0 °C. Freshly distilled trichlorosilane (3.31 mmol, 0.33 mL, 2.0 eq.) was added followed by dropwise addition of triethylamine (4.13 mmol, 0.58 mL, 2.5 eq.). In a separate flame-dried flask flushed with nitrogen was added α-boryl isocyanate (1.65 mmol, 0.50 g, 1.0 eq.) and triethylamine (4.13 mmol, 0.58 mL, 2.5 eq.) in DCM (8 mL) and the flask was cooled to 0 °C. The α-boryl isocyanate solution was slowly transferred to the trichlorosilane flask via cannula while maintaining the temperature at 0 °C. The resulting suspension was stirred vigorously at 0°C for 30 min. The resulting solution was allowed to warm to rt. Stirring was continued until starting material was completely consumed as indicated by TLC or crude ^{1}H NMR. The reaction solution was cooled to 0 °C and then 1 mL of triethylamine was added. Next, saturated aq.

$NaHCO_3$ was added slowly. The resulting suspension was stirred at 0 °C until bubbling ceased at which point it was allowed to warm to rt. The DCM layer was removed *in vacuo*. The aqueous layer was extracted with EtOAc (x3). The combined organic layers were washed with saturated aq. $NaHCO_3/H_2O$ (50/50) and saturated aq. $NaHCO_3$/brine (50/50), dried over Na_2SO_4, filtered and concentrated. The crude residue was purified by flash column chromatography on neutralized silica using hexanes:ethyl acetate with 1% triethylamine to yield the desired product **2**. Characterization of **2a** matched previous literature reports.[17]

MIDA (1-isocyano-2-phenylethyl)boronate (2b). White solid; yield = 296 mg, 63%; R_f = 0.22 (4:1 DCM:Ace). ^{1}H NMR (500 MHz, Acetonitrile-d_3) δ 7.38 – 7.32 (m, 4H), 7.29 – 7.26 (m, 1H), 4.13 (dd, *J* = 17.2, 11.9 Hz, 2H), 3.98 (dd, *J* = 17.2, 9.9 Hz, 2H), 3.51 (brd, *J* = 11.4 Hz, 1H), 3.09 (s, 3H), 3.04 (dt, *J* = 14.2, 3.9 Hz, 1H), 2.80 (dd, *J* = 14.2, 11.9 Hz, 1H). ^{13}C NMR (126 MHz, Acetonitrile-d_3) δ 168.4, 168.4, 158.3 (t, *J* = 4.8 Hz), 139.9, 130.0, 129.3, 127.6, 63.9, 63.7, 47.2, 37.2. ^{11}B NMR (160 MHz, Acetonitrile-d_3) δ 10.1. HRMS (DART-TOF$^+$): *m/z* for $C_{14}H_{16}BN_2O_4$: calcd 287.1203, observed 287.1198 [M+H].

General procedure for the synthesis of racemic B(MIDA) compounds from boryl isocyanides (3). In a 20 mL vial equipped with a magnetic stir bar under nitrogen atmosphere, was added boryl isocyanide **2a** or **2b** (1.0 eq.), a carboxylic acid (2.0 eq.), an aldehyde (2.0 eq.) and ammonia (0.5 M in 1,4-dioxane, 2.0 eq.) in TFE (4 mL, 0.1 M). The reaction was allowed to stir at room temperature for up to 3 days or until the reaction went to completion. The reaction was monitored by TLC and LC-MS. The solvent was removed *in vacuo* and then loaded onto Celite. The crude mixture was purified by flash column chromatography or Combiflash using hexanes:ethyl acetate to afford ***syn*-3** and ***anti*-3** as pure diastereomers.

MIDA (1-(2-(2-chloro-4-methoxybenzamido)-4-methylpentanamido)-3-methylbutyl)boronate (3a). White solid; yield = 47 mg, 45% (1:1 dr); ***syn*-3a**: R_f = 0.18 (1:9 hex:EtOAc). ^{1}H NMR (500 MHz,

Acetonitrile-d_3) δ 7.41 (d, J = 8.6 Hz, 1H), 7.04 (brd, J = 7.0 Hz, 1H), 7.01 (d, J = 2.5 Hz, 1H), 6.90 (dd, J = 8.6, 2.5 Hz, 1H), 6.39 (brd, J = 10.2 Hz, 1H), 4.25 (ddd, J = 10.5, 7.1, 4.6 Hz, 1H), 4.19 (d, J = 16.6 Hz, 1H), 3.94 (d, J = 17.3 Hz, 1H), 3.90 (d, J = 16.6 Hz, 1H), 3.82 (d, J = 17.2 Hz, 1H), 3.82 (s, 3H), 3.67 (ddd, J = 12.0, 10.2, 3.1 Hz, 1H), 2.90 (s, 3H), 1.79 – 1.71 (m, 1H), 1.65 – 1.53 (m, 2H), 1.50 – 1.44 (m, 2H), 1.28 (ddd, J = 13.9, 10.5, 3.1 Hz, 1H), 0.94 (d, J = 6.5 Hz, 3H), 0.93 (d, J = 6.4 Hz, 3H), 0.90 (d, J = 6.7 Hz, 3H), 0.87 (d, J = 6.5 Hz, 3H). ^{13}C NMR (126 MHz, Acetonitrile-d_3) δ 173.1, 169.2, 169.0, 167.9, 162.2, 132.7, 131.6, 128.7, 116.2, 113.7, 63.7, 63.0, 56.5, 54.3, 46.6, 41.4, 41.0, 25.6, 25.2, 24.1, 23.4, 21.7, 21.4. ^{11}B NMR (160 MHz, Acetonitrile-d_3) δ 11.7. ***anti*-3a**: R_f = 0.14 (EtOAc). ^{1}H NMR (500 MHz, Acetonitrile-d_3) δ 7.50 (d, J = 8.6 Hz, 1H), 7.01 (m, 2H), 6.92 (dd, J = 8.6, 2.5 Hz, 1H), 6.25 (brd, J = 10.1 Hz, 1H), 3.94 (d, J = 17.2 Hz, 1H), 3.92 (d, J = 16.8 Hz, 1H), 3.86 (d, J = 17.2 Hz, 1H), 3.83 (s, 3H), 3.77 (d, J = 16.8 Hz, 1H), 3.73 – 3.67 (m, 1H), 2.96 (s, 3H), 1.76 (ddq, J = 13.0, 7.5, 6.6 Hz, 1H), 1.62 – 1.59 (m, 2H), 1.56 (dp, J = 10.2, 3.5 Hz, 1H), 1.45 (ddd, J = 14.1, 12.1, 3.3 Hz, 1H), 1.28 (ddd, J = 13.9, 10.5, 3.1 Hz, 2H), 0.94 (d, J = 6.6 Hz, 3H), 0.92 (d, J = 6.5 Hz, 4H), 0.88 (d, J = 6.7 Hz, 4H), 0.87 (d, J = 6.5 Hz, 4H). ^{13}C NMR (126 MHz, Acetonitrile-d_3) δ 172.5, 168.9, 168.9, 167.9, 162.4, 132.6, 132.0, 128.4, 116.1, 113.8, 63.5, 63.1, 56.5, 54.5, 46.7, 41.5, 41.3, 25.6, 25.0, 24.2, 23.3, 21.6, 21.5. ^{11}B NMR (160 MHz, Acetonitrile-d_3) δ 11.6. HRMS (ESI, positive): *m/z* for $C_{24}H_{36}BClN_3O_7$: calcd 523.2366, observed 523.2365 [M+H].

MIDA (1-(2-([1,1'-biphenyl]-2-carboxamido)-4-methylpentanamido)-3-methylbutyl)boronate (3b). White solid; yield = 90 mg, 92% (1:1 dr); ***syn*-3b**: R_f = 0.71 (EtOAc). ^{1}H NMR (500 MHz, Acetonitrile-d_3) δ 7.51 (td, J = 7.4, 1.7 Hz, 1H), 7.46 – 7.43 (m, 2H), 7.42 – 7.38 (m, 5H), 7.37 – 7.33 (m, 1H), 6.67 (brd, J = 6.7 Hz, 1H), 6.23 (brd, J = 10.2 Hz, 1H), 4.13 (d, J = 16.6 Hz, 1H), 3.99 (ddd, J = 11.0, 6.8, 4.1 Hz, 1H), 3.90 (d, J = 17.2 Hz, 1H), 3.82 (d, J = 16.5 Hz, 1H), 3.78 (d, J = 17.2 Hz, 1H), 3.63 (ddd, J = 12.0, 10.2, 3.1 Hz, 1H), 2.78 (s, 3H), 1.52 (dtt, J = 13.3, 6.6, 3.1 Hz, 1H), 1.48 – 1.33 (m, 2H), 1.28 – 1.23 (m, 2H), 1.20 – 1.10 (m, 1H), 0.87 (dd, J = 16.2, 6.6 Hz, 6H), 0.77 (dd, J = 15.6, 6.5 Hz, 6H). ^{13}C

NMR (126 MHz, Acetonitrile-d_3) δ 173.2, 171.1, 169.3, 168.9, 141.4, 140.7, 137.0, 131.1, 130.8, 129.5 (2C), 129.4 (2C), 129.1, 128.4, 128.2, 63.7, 62.9, 54.2, 46.45, 41.4, 40.8, 25.2, 25.0, 24.1, 23.5, 21.6, 21.4. ^{11}B NMR (128 MHz, Acetonitrile-d_3) δ 11.5. ***anti*-3b**: R_f = 0.53 (EtOAc). ^{1}H NMR (400 MHz, Acetonitrile-d_3) δ 7.56 (td, J = 7.4, 1.4 Hz, 1H), 7.52 (dd, J = 7.5, 1.5 Hz, 1H), 7.46 – 7.38 (m, 7H), 6.43 (brd, J = 6.3 Hz, 1H), 6.07 (brd, J = 10.2 Hz, 1H), 4.00 – 3.95 (m, 3H), 3.83 (dd, J = 17.0, 10.8 Hz, 2H), 3.67 (ddd, J = 12.9, 10.4, 3.1 Hz, 1H), 2.94 (s, 3H), 1.51 – 1.41 (m, 2H), 1.28 (dtd, J = 14.3, 11.1, 10.3, 6.3 Hz, 2H), 1.16 (ddd, J = 13.7, 10.2, 4.7 Hz, 1H), 1.03 – 0.91 (m, 1H), 0.85 (dd, J = 12.7, 6.5 Hz, 6H), 0.72 (dd, J = 16.9, 6.5 Hz, 6H). ^{13}C NMR (126 MHz, Acetonitrile-d_3) δ 172.6, 171.3, 169.1, 168.9, 141.5, 140.6, 136.6, 131.0, 131.0, 129.6 (2C), 129.4 (2C), 129.4, 128.5, 128.3, 63.5, 63.1, 54.6, 46.7, 41.4, 41.3, 25.0, 24.8, 24.1, 23.3, 21.9, 21.4. ^{11}B NMR (128 MHz, Acetonitrile-d_3) δ 11.5. HRMS (ESI, positive): *m/z* for $C_{29}H_{39}BN_3O_6$: calcd 535.2963, observed 535.2962 [M+H].

MIDA (1-(2-(4-fluoro-3-nitrobenzamido)-4-methylpentanamido)-3-methylbutyl)boronate (3c). Yellow solid; yield = 62 mg, 61% (1:1 dr); ***syn*-3c**: R_f = 0.19 (1:9 hex:EtOAc). ^{1}H NMR (500 MHz, Acetonitrile-d_3) δ 8.49 (ddd, J = 7.2, 2.3, 1.2 Hz, 1H), 8.15 (ddd, J = 8.7, 4.2, 2.3 Hz, 1H), 7.52 – 7.45 (m, 2H), 6.43 (brd, J = 9.7 Hz, 1H), 4.31 – 4.27 (m, 1H), 4.15 (d, J = 16.6 Hz, 1H), 3.95 (dd, J = 10.1, 1.2 Hz, 1H), 3.92 (dd, J = 9.5, 1.2 Hz, 1H), 3.83 (dd, J = 17.2, 1.1 Hz, 1H), 3.66 (ddd, J = 12.0, 10.1, 3.1 Hz, 1H), 2.87 (s, 3H), 1.81 – 1.70 (m, 2H), 1.60 – 1.44 (m, 3H), 1.28 (ddd, J = 13.9, 10.4, 3.1 Hz, 1H), 0.97 (d, J = 6.4 Hz, 3H), 0.92 (d, J = 6.5 Hz, 4H), 0.90 (d, J = 6.7 Hz, 3H), 0.87 (d, J = 6.5 Hz, 3H). ^{13}C NMR (126 MHz, Acetonitrile-d_3) δ 173.1, 169.2, 169.0, 165.6, 157.9 (d, $^1J_{C\text{-}F}$ = 266.7 Hz), 138.0 (d, $^4J_{C\text{-}F}$ = 8.0 Hz), 135.9 (d, $^3J_{C\text{-}F}$ = 10.0 Hz), 131.9 (d, $^2J_{C\text{-}F}$ = 3.9 Hz), 126.5 (d, $^3J_{C\text{-}F}$ = 2.0 Hz), 119.6 (d, $^2J_{C\text{-}F}$ = 21.6 Hz), 63.7, 63.0, 54.7, 46.4, 41.4, 40.8, 25.6, 25.3, 24.1, 23.4, 21.7, 21.5. ^{11}B NMR (128 MHz, Acetonitrile-d_3) δ 11.8. ^{19}F NMR (470 MHz, Acetonitrile-d_3) δ -115.7 (ddd, J = 11.2, 7.3, 4.0 Hz). ***anti*-3c**: R_f = 0.19 (EtOAc). ^{1}H NMR (400 MHz, Acetonitrile-d_3) δ 8.56 (dd, J = 7.2, 2.3 Hz, 1H), 8.19 (ddd, J = 8.7, 4.3, 2.3 Hz, 1H), 7.49 (dd, J = 10.9, 8.8 Hz, 1H), 7.47 (brd, J = 6.5 Hz, 1H), 6.23 (brd, J = 10.1

Hz, 1H), 4.31 (ddd, *J* = 9.6, 6.6, 5.3 Hz, 1H), 3.95 – 3.73 (m, 4H), 3.68 (ddd, *J* = 12.1, 10.2, 3.3 Hz, 1H), 2.96 (s, 3H), 1.80 – 1.73 (m, 1H), 1.71 – 1.63 (m, 2H), 1.53 (ddt, *J* = 13.4, 6.5, 3.6 Hz, 1H), 1.46 (ddd, *J* = 14.0, 12.1, 3.2 Hz, 1H), 1.28 – 1.23 (m, 1H), 0.96 (d, *J* = 6.5 Hz, 3H), 0.90 (d, *J* = 6.5 Hz, 3H), 0.86 (dd, *J* = 6.6, 5.6 Hz, 6H). ^{13}C NMR (126 MHz, Acetonitrile-d_3) δ 172.6, 169.1, 168.7, 165.8, 158.0 (d, *J* = 266.8 Hz), 136.2 (d, *J* = 10.0 Hz), 131.6 (d, *J* = 3.8 Hz), 126.8 (d, *J* = 2.1 Hz), 119.5 (d, *J* = 21.6 Hz), 63.6, 63.1, 55.3, 46.78, 41.1, 41.1, 25.6, 25.0, 24.1, 23.1, 21.7, 21.4. ^{11}B NMR (128 MHz, Acetonitrile-d_3) δ 11.6. ^{19}F NMR (377 MHz, Acetonitrile-d_3) δ -115.5 (q, *J* = 5.6 Hz). HRMS (ESI, positive): *m/z* for $C_{23}H_{33}BFN_4O_8$: calcd 522.2406, observed 522.2397 [M+H].

MIDA (3-methyl-1-(4-methyl-2-(1-phenylcyclopropane-1-carboxamido)pentanamido)butyl)boronate (3d). White solid; yield = 48 mg, 80% (1:1 dr); ***syn*-3d**: R_f = 0.33 (EtOAc). ^{1}H NMR (500 MHz, Acetonitrile-d_3) δ 7.43 – 7.36 (m, 4H), 7.36 – 7.30 (m, 1H), 6.26 (brd, *J* = 10.1 Hz, 1H), 5.76 (brd, *J* = 7.3 Hz, 1H), 4.08 (q, *J* = 7.4 Hz, 1H), 4.05 (d, *J* = 16.6 Hz, 1H), 3.96 (d, *J* = 17.2 Hz, 1H), 3.90 (d, *J* = 16.6 Hz, 1H), 3.83 (d, *J* = 17.2 Hz, 1H), 3.60 (ddd, *J* = 11.9, 10.0, 3.1 Hz, 1H), 2.85 (s, 3H), 1.50 (ddq, *J* = 13.3, 6.6, 3.2 Hz, 1H), 1.45 (ddd, *J* = 9.8, 6.4, 3.2 Hz, 1H), 1.41 (dd, *J* = 5.3, 1.8 Hz, 1H), 1.40 – 1.38 (m, 1H), 1.36 (dt, *J* = 6.6, 3.3 Hz, 1H), 1.34 – 1.30 (m, 2H), 1.25 (ddd, *J* = 13.9, 10.5, 3.1 Hz, 1H), 1.06 (ddd, *J* = 9.7, 6.4, 3.2 Hz, 1H), 1.00 (ddd, *J* = 9.4, 6.4, 3.2 Hz, 1H), 0.88 (d, *J* = 6.7 Hz, 3H), 0.83 (d, *J* = 6.5 Hz, 3H), 0.81 (d, *J* = 1.3 Hz, 3H), 0.80 (d, *J* = 1.3 Hz, 3H). ^{13}C NMR (126 MHz, Acetonitrile-d_3) δ 174.7, 172.9, 169.2, 169.0, 140.6, 131.6 (2C), 129.9 (2C), 128.8, 63.7, 63.0, 54.1, 46.4, 41.4, 41.0, 31.0, 25.6, 25.2, 24.1, 23.3, 22.0, 21.4, 15.8, 15.7. ^{11}B NMR (128 MHz, Acetonitrile-d_3) δ 11.5. ***anti*-3d**: R_f = 0.14 (EtOAc). ^{1}H NMR (500 MHz, Acetonitrile-d_3) δ 7.46 – 7.44 (m, 2H), 7.42 – 7.38 (m, 2H), 7.36 – 7.33 (m, 1H), 5.93 (brd, *J* = 10.3 Hz, 1H), 5.79 (brd, *J* = 6.7 Hz, 1H), 4.07 – 4.03 (m, 1H), 3.95 (d, *J* = 17.2 Hz, 1H), 3.94 (d, *J* = 16.7 Hz, 1H), 3.84 (d, *J* = 17.2 Hz, 1H), 3.72 (d, *J* = 16.8 Hz, 1H), 3.61 (ddd, *J* = 12.1, 10.2, 3.1 Hz, 1H), 2.88 (s, 3H), 1.48 – 1.20 (m, 8H), 1.10 (ddd, *J* = 7.6, 5.8, 2.8 Hz, 1H), 0.99 (ddd, *J* = 9.4, 5.9, 2.5 Hz, 1H), 0.87 (d, *J* = 6.7 Hz, 3H), 0.83

(d, J = 6.5 Hz, 3H), 0.81 (d, J = 4.4 Hz, 3H), 0.80 (d, J = 4.3 Hz, 3H). ^{13}C NMR (126 MHz, Acetonitrile-d_3) δ 175.3, 172.8, 169.0, 168.8, 140.4, 132.0 (2C), 129.9 (2C), 128.8, 63.6, 63.2, 54.9, 46.67, 41.5, 40.9, 31.0, 25.6, 24.9, 24.1, 23.2, 21.7, 21.4, 16.5, 16.0. ^{11}B NMR (128 MHz, Acetonitrile-d_3) δ 11.6. HRMS (DART, TOF$^+$): *m/z* for $C_{26}H_{39}BN_3O_6$: calcd 500.2931, observed 500.2928 [M+H].

MIDA (1-(2-(2-hydroxy-5-methoxybenzamido)-4-methylpentanamido)-3-methylbutyl)boronate (3e). White solid; yield = 74 mg, 63% (1:1 dr); ***syn*-3e**: R_f = 0.53 (EtOAc). ^{1}H NMR (400 MHz, Acetonitrile-d_3) δ 11.55 (brs, 1H), 7.69 (brd, J = 6.9 Hz, 1H), 7.19 (d, J = 3.0 Hz, 1H), 6.99 (dd, J = 9.0, 3.0 Hz, 1H), 6.83 (d, J = 9.0 Hz, 1H), 6.52 (brd, J = 10.1 Hz, 1H), 4.37 (ddd, J = 10.2, 6.9, 4.7 Hz, 1H), 4.03 (d, J = 16.3 Hz, 1H), 3.98 (d, J = 3.6 Hz, 1H), 3.93 (d, J = 2.9 Hz, 1H), 3.83 (d, J = 17.2 Hz, 1H), 3.76 (s, 3H), 3.69 (ddd, J = 11.9, 10.1, 3.0 Hz, 1H), 2.89 (s, 3H), 1.81 – 1.72 (m, 2H), 1.63 – 1.53 (m, 1H), 1.53 – 1.43 (m, 1H), 1.29 (ddd, J = 13.8, 10.4, 3.0 Hz, 1H), 0.96 (d, J = 6.3 Hz, 3H), 0.91 (d, J = 6.4 Hz, 3H), 0.89 (d, J = 6.7 Hz, 3H), 0.88 (d, J = 6.5 Hz, 3H). ^{13}C NMR (126 MHz, Acetonitrile-d_3) δ 172.9, 171.1, 169.1, 168.8, 156.1, 152.9, 122.7, 119.6, 115.0, 111.3, 63.5, 63.0, 56.6, 54.2, 46.4, 41.3, 40.8, 25.6, 25.3, 24.1, 23.4, 21.6, 21.4. ^{11}B NMR (128 MHz, Acetonitrile-d_3) δ 11.8. ***anti*-3e**: R_f = 0.10 (EtOAc). ^{1}H NMR (400 MHz, Acetonitrile-d_3) δ 11.37 (brs, 1H), 7.55 (brd, J = 6.9 Hz, 1H), 7.20 (d, J = 3.0 Hz, 1H), 7.04 (dd, J = 9.0, 3.0 Hz, 1H), 6.86 (d, J = 9.0 Hz, 1H), 6.26 (brd, J = 10.1 Hz, 1H), 4.40 (ddd, J = 9.8, 6.9, 5.0 Hz, 1H), 3.94 (d, J = 17.4 Hz, 1H), 3.88 – 3.81 (m, 1H), 3.78 (s, 3H), 3.72 – 3.66 (m, 1H), 3.67 (d, J = 16.8 Hz, 1H), 2.95 (s, 3H), 1.79 – 1.68 (m, 2H), 1.66 – 1.60 (m, 1H), 1.59 – 1.51 (m, 1H), 1.46 (ddd, J = 14.1, 12.0, 3.3 Hz, 1H), 1.26 (ddd, J = 13.9, 10.5, 3.1 Hz, 1H), 0.95 (d, J = 6.2 Hz, 3H), 0.90 (d, J = 6.3 Hz, 3H), 0.86 (d, J = 4.2 Hz, 3H), 0.85 (d, J = 4.0 Hz, 3H). ^{13}C NMR (126 MHz, Acetonitrile-d_3) δ 172.7, 170.9, 169.1, 168.5, 155.8, 152.8, 122.5, 119.4, 115.0, 111.8, 63.5, 63.0, 56.6, 54.4, 46.7, 41.3, 41.0, 25.6, 25.0, 24.1, 23.1, 21.7, 21.4. ^{11}B NMR (128 MHz, Acetonitrile-d_3) δ 11.7. HRMS (ESI, positive): *m/z* for $C_{24}H_{37}BN_3O_8$: calcd 505.2705, observed 505.2701 [M+H].

MIDA (1-(2-(2-chloro-4-methoxybenzamido)-4-methylpentanamido)-2-phenylethyl)boronate (3f). White solid; yield = 78 mg, 40% (1:1 dr); ***syn*-3f**: R_f = 0.11 (EtOac). ^{1}H NMR (500 MHz, Acetonitrile-d_3) δ 7.37 (d, *J* = 8.6 Hz, 1H), 7.25 – 7.21 (m, 4H), 7.17 – 7.14 (m, 1H), 6.98 (d, *J* = 2.5 Hz, 1H), 6.88 (d, *J* = 2.5 Hz, 1H), 6.87 (d, *J* = 2.5 Hz, 1H), 6.81 (brd, *J* = 6.9 Hz, 1H), 6.48 (brd, *J* = 10.2 Hz, 1H), 4.26 (d, *J* = 16.6 Hz, 1H), 4.03 (ddd, *J* = 10.9, 7.0, 4.3 Hz, 1H), 3.98 (d, *J* = 17.2 Hz, 1H), 3.95 – 3.90 (m, 1H), 3.92 (d, *J* = 16.6 Hz, 1H), 3.86 (d, *J* = 17.2 Hz, 1H), 3.80 (s, 3H), 3.02 (dd, *J* = 14.1, 3.5 Hz, 1H), 2.92 (s, 3H), 2.61 (dd, *J* = 14.1, 12.3 Hz, 1H), 1.41 (dddd, *J* = 13.2, 11.5, 9.4, 6.6 Hz, 1H), 1.13 (ddd, *J* = 14.0, 10.7, 5.0 Hz, 1H), 0.85 (td, *J* = 9.5, 4.7 Hz, 1H), 0.81 (d, *J* = 4.9 Hz, 3H), 0.80 (d, *J* = 4.9 Hz, 3H). ^{13}C NMR (126 MHz, Acetonitrile-d_3) δ 172.9, 169.3, 168.9, 167.9, 162.2, 141.2, 132.7, 131.6, 130.4 (2C), 128.9 (2C), 126.7, 116.2, 113.6, 63.8, 63.0, 56.5, 54.2, 46.6, 40.5, 38.0, 25.3, 23.4, 21.6. ^{11}B NMR (128 MHz, Acetonitrile-d_3) δ 11.6. ***anti*-3f**: R_f = 0.08 (EtOAc). ^{1}H NMR (500 MHz, Acetonitrile-d_3) δ 7.51 (d, *J* = 8.7 Hz, 1H), 7.25 – 7.20 (m, 4H), 7.17 – 7.12 (m, 1H), 7.02 (d, *J* = 2.5 Hz, 1H), 6.94 (dd, *J* = 8.6, 2.5 Hz, 1H), 6.77 (brd, *J* = 6.6 Hz, 1H), 6.23 (brd, *J* = 9.8 Hz, 1H), 4.15 (ddd, *J* = 9.8, 6.5, 5.1 Hz, 1H), 3.98-3.96 (m, 1H), 3.92 (d, *J* = 16.3 Hz, 2H), 3.88 (d, *J* = 5.6 Hz, 2H), 3.85 (s, 3H), 3.81 (d, *J* = 16.7 Hz, 2H), 2.99 (s, 3H), 1.59 (dddd, *J* = 13.2, 12.0, 9.0, 6.6 Hz, 1H), 1.25 – 1.22 (m, 2H), 0.87 (d, *J* = 6.6 Hz, 3H), 0.83 (d, *J* = 6.5 Hz, 3H). ^{13}C NMR (126 MHz, Acetonitrile-d_3) δ 172.6, 168.9, 168.9, 168.2, 163.0, 141.4, 132.6, 130.7, 130.7, 129.2, 129.1, 127.1, 116.6, 114.3, 64.0, 63.6, 56.9, 55.2, 47.2, 41.8, 38.6, 25.9, 23.5, 21.9. ^{11}B NMR (128 MHz, Acetonitrile-d_3) δ 11.4. HRMS (ESI, positive): *m/z* for $C_{27}H_{34}BClN_3O_7$: calcd 557.2209, observed 557.2204 [M+H].

General procedure for the synthesis of racemic boronic acids (4). In a small vial equipped with a magnetic stir bar under nitrogen atmosphere, was added MIDA boronate ***syn*-3** or ***anti*-3** (1.0 eq.) and HCl (1.25 M in MeOH, 10 eq.), in MeOH (0.5 M). The reaction was left to stir overnight at room temperature. The reaction was monitored by TLC and LC-MS. Upon completion, the solvent was removed under a gentle stream of nitrogen. The crude mixture was loaded onto Celite and purified by

flash column chromatography* [Acetone → MeCN → DCM:MeOH (10:1)] to afford pure product. The pure compound was dissolved in MeCN:H_2O (1:1) and lyophilized to provide the boronic acid ***syn*-4** or ***anti*-4** as a fluffy white solid. The racemic boronic acids were checked for purity by LC-MS prior to assay submission. Full characterization were provided for the enantiopure boronic acids instead.

Note: The boronic acids are streak on silica gel and reverse-phase C18. In order to recover appreciable amounts of boronic acid using normal-phase column chromatography, it is necessary to flush with ~6-8 column volumes of 15% MeOH in DCM. It is also important to use a smaller diameter column (~1 cm for 100 mg of starting material) to prevent the product from eluting too dilute.

Synthesis of (1*R*)-(*S*)-pinanediol 1-ammonium-3-methylbutane-1-boronate trifluoroacetate salt (5a). (1*R*)-(*S*)-pinanediol 1-ammonium-3-methylbutane-1-boronate trifluoroacetate salt was prepared using a modified procedure.[4] In a 100 mL round-bottom flask equipped with a magnetic stir bar under nitrogen atmosphere, was added (2-methylpropyl)boronic acid (2.50 g, 24.5 mmol, 1.0 eq.), (1*S*,2*S*,3*R*,2*S*)-(+)-pinanediol (4.58 g, 26.9 mmol, 1.1 eq.) and $MgSO_4$ (ca. 5 g) in Et_2O (24.5 mL, 1.0 M). The reaction was left to stir at room temperature overnight. The reaction was monitored by TLC. Upon completion, the mixture was filtered and the solvent was removed *in vacuo*. The crude oil was purified by flash column chromatography using hexanes:Et_2O to afford pure (*S*)-pinanediol-2-methylpropane-1-boronate in 87% yield. Characterization matched previous literature reports.[3] In a flame-dried, 250 mL two-neck round-bottom flask equipped with a magnetic stir bar under nitrogen atmosphere, was added (*S*)-pinanediol-2-methylpropane-1-boronate (5.00 g, 21.2 mmol, 1.0 eq.) and DCM (9.38 g, 110.4 mmol, 5.2 eq.) in THF (30 mL). The flask was cooled to -60 ºC. In a second flame-dried, round-bottom flask under nitrogen atmosphere, was added freshly distilled diisopropylamine (3.9 mL, 27.6 mmol, 1.3 eq.) in THF (15 mL). The flask was cooled to -10 ºC. nBuLi (10.5 mL, 26.3 mmol, 2.5 M in hexanes, 1.24 eq.) was added to diisopropylamine over 15 min while maintaining the temperature at -10 ºC. The LDA-mixture was stirred for 15 min -10 ºC before it was used. In a third

flame-dried, round-bottom flask under nitrogen atmosphere, was added $ZnCl_2$ (5.0 g, 37.1 mmol, 1.75 eq.) in THF (34 mL). The reaction flask was heated to 40 ºC and stirred for 1 h and 15 min before it was used. The LDA-mixture was added over 15 min to flask containing (*S*)-pinanediol-2-methylpropane-1-boronate, while maintaining the temperature at -60 ºC. A THF rinse (6 mL) was used to complete the addition. The reaction mixture was stirred for another 10 min at -60 ºC. The reaction mixture was warmed to -50 ºC over 5 min. The $ZnCl_2$-mixture was added over 15 min to the flask containing (*S*)-pinanediol-2-methylpropane-1-boronate and LDA-mixture, while maintaining the temperature at -50 ºC. A THF rinse (6 mL) was used to complete the addition. The reaction mixture was stirred for 15 min at -45 ºC and then warmed to 10 ºC over 30 min. 10% (v/v) H_2SO_4 solution (30 mL) was added over 10 min, while maintaining the temperature at 10 ºC to 20 ºC. The reaction was stirred for 5 minutes at room temperature before the aqueous phase was separated. The organic phase was washed with deionized water (15 mL) and then with 10% (w/v) NaCl solution (15 mL). The organic phase was collected and dried over Na_2SO_4. The organic layer was filtered and then the solvent was removed *in vacuo* to afford crude (1*S*)-(*S*)-pinanediol 1-chloro-3-methylbutane-1-boronate which was used in the next step without further purification. If the reaction did not go to completion, the crude mixture can still be carried through to the next step. In a flame-dried, round-bottom flask equipped with a magnetic stir bar under nitrogen atmosphere, was added crude (1*S*)-(*S*)-pinanediol 1-chloro-3-methylbutane-1-boronate (3.53 g, 12.4 mmol, 1.0 eq.) in THF (19 mL). It is possible to extrapolate the amount of (1*S*)-(*S*)-pinanediol 1-chloro-3-methylbutane-1-boronate in the crude mixture using ^{1}H NMR. In a second flame-dried, 150 mL two-neck round-bottom flask under nitrogen atmosphere, was added LiHMDS (11.9 mL, 1.0 M in THF, 0.96 eq.). The flask was cooled to -20 ºC. The crude (1*S*)-(*S*)-pinanediol 1-chloro-3-methylbutane-1-boronate in THF was added over 30 min to the flask containing the LiHMDS, while maintaining the temperature at -18 ºC. A THF rinse (1.7 mL) was used to complete the addition. The reaction was stirred for an additional 30 min at -15 ºC and then warmed to room temperature over 15 min. The solvent was

removed *in vacuo*. The crude oil was re-dissolved in Et_2O (40 mL) and the solids were filtered over a pad of Celite. The filtrate was collected and filtered through a plug of silica. The silica plug was washed with Et_2O (500 mL). The solvent was removed *in vacuo* to afford (1*R*)-(*S*)-pinanediol 1-bis(trimethylsilyl)amino-3-methylbutane-1-boronate as a crude oil. In a 250 mL round-bottom flask equipped with a magnetic stir bar under a nitrogen atmosphere, was added trifluoroacetic acid (1.9 mL, 25 mmol, 2.0 eq.) in Et_2O (25 mL). The flask was cooled to -10 ºC. In a separate round-bottom flask under nitrogen atmosphere, was added (1*R*)-(*S*)-pinanediol 1-bis(trimethylsilyl)amino-3-methylbutane-1-boronate (5.07 g, 12.4 mmol, 1.0 eq.) in Et_2O (25 mL). The (1*R*)-(*S*)-pinanediol 1-bis(trimethylsilyl)amino-3-methylbutane-1-boronate mixture was added over 15 min to the flask containing trifluoroacetic acid causing product precipitation, while maintaining the temperature at -10 ºC. An Et_2O rinse was used to complete the addition. The reaction mixture was stirred overnight at 4 ºC. The solid was collected by vacuum filtration and washed with Et_2O to afford pure (1*R*)-(*S*)-pinanediol 1-ammonium-3-methylbutane-1-boronate trifluoroacetate salt **5a**.

(1*R*)-(*S*)-pinanediol 1-ammonium-3-methylbutane-1-boronate trifluoroacetate salt (5a). White solid; yield = 1.309 g, 18%; LC-MS retention time = 3.23 min (Method A) ^{1}H NMR (600 MHz, Chloroform-*d*) δ 7.77 (brs, 3H), 4.33 (dd, *J* = 8.8, 1.8 Hz, 1H), 2.91 (brd, *J* = 6.4 Hz, 1H), 2.31 – 2.26 (m, 1H), 2.24 – 2.19 (m, 1H), 2.03 (dd, *J* = 6.0, 4.9 Hz, 1H), 1.91 – 1.86 (m, 2H), 1.79 (dt, *J* = 13.5, 6.8 Hz, 1H), 1.65 – 1.56 (m, 2H), 1.38 (s, 3H), 1.27 (s, 3H), 1.07 (d, *J* = 11.2 Hz, 1H), 0.92 (d, *J* = 5.7 Hz, 3H), 0.91 (d, *J* = 5.7 Hz, 3H), 0.81 (s, 3H). ^{13}C NMR (151 MHz, Chloroform-*d*) δ 162.3 (q, *J* = 35.7 Hz), 116.5 (q, *J* = 291.8 Hz), 87.8, 78.9, 51.2, 39.5, 38.6, 3836, 34.9, 28.2, 27.1, 26.4, 24.8, 24.0, 22.4, 22.2. ^{11}B NMR (192 MHz, Chloroform-*d*) δ 31.2. ^{19}F NMR (564 MHz, Chloroform-*d*) δ -75.6. HRMS (DART-TOF$^+$): *m/z* for $C_{15}H_{29}BNO_2$: calcd 266.2291, observed 266.2285 [M+H].

Synthesis of (1*S*)-(*R*)-pinanediol 1-ammonium-3-methylbutane-1-boronate trifluoroacetate salt (5b). Compound **5b** was prepared in an analogous manner to **5a**, except (1*R*,2*R*,3*S*,2*R*)-(-)-pinanediol was used instead for the preparation of (*S*)-pinanediol-2-methylpropane-1-boronate in 99% yield.

(1*S*)-(*R*)-pinanediol 1-ammonium-3-methylbutane-1-boronate trifluoroacetate salt (5b). White solid; yield = 3.556 g, 65%; LC-MS retention time = 3.43 min (Method A) ^{1}H NMR (400 MHz, Chloroform-*d*) δ 7.78 (brs, 3H), 4.32 (dd, *J* = 8.7, 1.8 Hz, 1H), 2.90 (t, *J* = 7.9 Hz, 1H), 2.33 – 2.17 (m, 2H), 2.03 (dd, *J* = 6.0, 4.8 Hz, 1H), 1.93 – 1.85 (m, 2H), 1.78 (dt, *J* = 13.3, 6.7 Hz, 1H), 1.63 – 1.57 (m, 2H), 1.39 (s, 3H), 1.28 (s, 3H), 1.07 (d, *J* = 11.1 Hz, 1H), 0.92 (d, *J* = 4.2 Hz, 3H), 0.91 (d, *J* = 4.2 Hz, 3H), 0.82 (s, 3H). ^{13}C NMR (126 MHz, Chloroform-*d*) δ 162.5 (q, *J* = 35.1 Hz), 116.7 (q, *J* = 292.8 Hz), 87.7, 78.8, 51.2, 39.5, 38.6, 38.2, 35.9 (C-B), 34.9, 28.2, 27.1, 26.3, 24.8, 24.0, 22.4, 22.2. ^{11}B NMR (128 MHz, Chloroform-*d*) δ 30.9. ^{19}F NMR (564 MHz, Chloroform-*d*) δ -75.6. HRMS (DART-TOF^{+}): *m/z* for $C_{15}H_{29}BNO_2$: calcd 266.2291, observed 266.2298 [M+H].

General procedure for the enantioselective synthesis of pinanediol boronates (7). The corresponding carboxylic acids were prepared by standard Fmoc solid-phase synthesis using 2-chlorotrityl chloride resin, single coupling steps with HATU and cleavage steps with 25% HFIP in DCM (x3). For a list of carboxylic acids **6a-6d**, see Supporting Information. The enantiopure pinanediol boronates were prepared using a modified procedure.[40] In a 20 mL vial equipped with a magnetic stir bar under nitrogen atmosphere, was added carboxylic acid **6** (1.0 eq.), (1*R*)-(*S*)-pinanediol 1-ammonium-3-methylbutane-1-boronate trifluoroacetate salt **5a** or (1*S*)-(*R*)-pinanediol 1-ammonium-3-methylbutane-1-boronate trifluoroacetate salt **5b** (1.05 eq.) and TBTU (1.1 eq.) in DCM (0.17 M). The flask was cooled to 4 ºC and then diisopropylethylamine (3.0 eq.) was added slowly. The reaction mixture was allowed to stir at 0 ºC until completion. The reaction was monitored by TLC and LC-MS. Upon reaction completion, the solvent was removed *in vacuo*. The crude mixture was re-dissolved in EtOAc and washed with deionized H_2O, 1% (v/v) H_3PO_4, 2% (w/v) K_2CO_3 and 10% (w/v) NaCl solution. The organic layer was collected,

dried over Na_2SO_4 and filtered. The filtrate was collected and the solvent was removed *in vacuo*. The crude mixture was loaded onto Celite and purified by reverse-phase column chromatography using H_2O:MeCN to afford pure pinanediol boronates **7**. The diastereomeric ratio was determined by HPLC using Method B or Method C.

(+)-Pinanediol ((*R*)-1-((*S*)-2-(2-chloro-4-methoxybenzamido)-4-methylpentanamido)-3-methylbutyl)boronate (7a). White solid; yield = 156 mg, 95% (>95:5 dr); R_f = 0.22 (30% EtOAc in hexanes). ^{1}H NMR (600 MHz, Chloroform-*d*) δ 7.63 (d, *J* = 8.7 Hz, 1H), 6.89 (d, *J* = 2.5 Hz, 1H), 6.82 (dd, *J* = 8.7, 2.5 Hz, 1H), 6.76 (d, *J* = 8.3 Hz, 1H), 6.55 (s, 1H), 4.68 (td, *J* = 8.4, 5.9 Hz, 1H), 4.29 (dd, *J* = 8.8, 2.1 Hz, 1H), 3.82 (s, 3H), 3.22 (dt, *J* = 9.2, 5.9 Hz, 1H), 2.38 – 2.26 (m, 1H), 2.22 – 2.11 (m, 1H), 2.00 (dd, *J* = 6.0, 5.1 Hz, 1H), 1.88 (td, *J* = 5.7, 2.9 Hz, 1H), 1.84 (ddd, *J* = 14.5, 3.3, 2.1 Hz, 1H), 1.81 – 1.70 (m, 2H), 1.68 – 1.61 (m, 2H), 1.52 – 1.41 (m, 2H), 1.38 (s, 3H), 1.27 (s, 3H), 1.24 (m, 1H), 0.96 (d, *J* = 6.5 Hz, 3H), 0.95 (d, *J* = 6.3 Hz, 3H), 0.90 (d, *J* = 5.5 Hz, 3H), 0.89 (d, *J* = 5.6 Hz, 3H), 0.83 (s, 3H). ^{13}C NMR (151 MHz, Chloroform-*d*) δ 166.1, 161.7, 132.1, 132.0, 126.5, 115.6, 113.2, 85.7, 77.9, 60.5, 55.8, 51.7, 51.6, 41.1, 40.3, 39.8, 38.3, 35.8, 28.8, 27.3, 26.5, 25.7, 24.9, 24.2, 23.2, 23.0, 22.4, 22.2. ^{11}B NMR (160 MHz, Chloroform-*d*) δ 29.3. HRMS (DART-TOF$^+$): *m/z* for $C_{29}H_{45}BClN_2O_5$: calcd 547.3110, observed 547.3113 [M+H].

(+)-Pinanediol ((*R*)-1-((*S*)-2-([1,1'-biphenyl]-2-carboxamido)-4-methylpentanamido)-3-methylbutyl)boronate (7b). White solid; yield = 243 mg, 79% (>95:5 dr); R_f = 0.36 (30% EtOAc in hexanes). ^{1}H NMR (500 MHz, Chloroform-*d*) δ 7.62 (dt, *J* = 7.7, 2.0 Hz, 1H), 7.47 (td, *J* = 7.5, 1.4 Hz, 1H), 7.44 – 7.32 (m, 7H), 6.34 (d, *J* = 5.2 Hz, 1H), 5.66 (d, *J* = 8.2 Hz, 1H), 4.39 (td, *J* = 8.2, 6.1 Hz, 1H), 4.26 (dd, *J* = 8.8, 2.2 Hz, 1H), 3.12 (td, *J* = 7.6, 5.2 Hz, 1H), 2.30 (ddt, *J* = 14.0, 8.7, 2.4 Hz, 1H), 2.14 (dtd, *J* = 10.7, 6.2, 2.3 Hz, 1H), 1.99 (t, *J* = 5.6 Hz, 1H), 1.87 (tt, *J* = 5.6, 3.0 Hz, 1H), 1.81 (ddd, *J* = 14.4, 3.3, 2.1 Hz, 1H), 1.63 (hept, *J* = 6.7 Hz, 1H), 1.45 – 1.42 (m, 1H), 1.42 – 1.39 (m, 3.6 Hz, 1H), 1.35 (s, 3H), 1.27 (s, 3H), 1.22 (d, *J* = 10.7 Hz, 1H), 1.20 – 1.08 (m, 3H), 0.91 (d, *J* = 6.8 Hz, 3H), 0.89

(d, J = 6.6 Hz, 3H), 0.83 (d, J = 0.0 Hz, 3H), 0.78 (d, J = 2.7 Hz, 3H), 0.77 (dd, J = 2.6, 0.0 Hz, 3H). ^{13}C NMR (126 MHz, Chloroform-*d*) δ 172.2, 169.6, 140.4, 139.8, 135.3, 130.5, 130.4, 128.9 (2C), 128.8 (2C), 128.7, 127.9, 127.7, 85.6, 77.8, 51.6, 51.2, 40.4, 40.3, 39.8, 38.3, 35.8, 28.7, 27.3, 26.4, 25.6, 24.3, 24.2, 23.1, 22.9, 22.4, 22.3. ^{11}B NMR (160 MHz, Chloroform-*d*) δ 28.7. HRMS (DART-TOF$^+$): *m/z* for $C_{34}H_{48}BN_2O_4$: calcd 559.3707, observed 559.3713 [M+H].

(+)-Pinanediol ((*R*)-1-((*S*)-2-(4-fluoro-3-nitrobenzamido)-4-methylpentanamido)-3-methylbutyl)boronate (7c). Yellow solid; yield = 123 mg, 37% (>95:5 dr); R_f = 0.32 (30% EtOAc in hexanes). ^{1}H NMR (600 MHz, Chloroform-*d*) δ 8.49 (dd, J = 6.9, 2.3 Hz, 1H), 8.09 (ddd, J = 8.7, 4.1, 2.3 Hz, 1H), 7.36 (dd, J = 10.1, 8.6 Hz, 1H), 7.03 (brs, 1H), 6.12 (brs, 1H), 4.66 – 4.61 (m, 1H), 4.32 (dd, J = 8.8, 2.1 Hz, 1H), 3.36 – 3.33 (m, 1H), 2.34 (ddt, J = 14.2, 8.8, 2.5 Hz, 1H), 2.19 (dtd, J = 10.8, 6.0, 2.1 Hz, 1H), 2.01 (t, J = 5.5 Hz, 1H), 1.92 (dq, J = 5.7, 3.0 Hz, 1H), 1.84 (ddd, J = 14.5, 3.3, 2.1 Hz, 1H), 1.77 – 1.61 (m, 4H), 1.48 (td, J = 7.7, 7.1, 2.1 Hz, 2H), 1.39 (s, 3H), 1.29 (s, 3H), 1.20 (d, J = 10.9 Hz, 1H), 0.98 (d, J = 6.3 Hz, 3H), 0.96 (d, J = 6.0 Hz, 3H), 0.90 (t, J = 6.3 Hz, 6H), 0.84 (s, 3H). ^{13}C NMR (126 MHz, Chloroform-*d*) δ 172.2, 164.0, 157.2 (d, $^1J_{C\text{-}F}$ = 270.1 Hz), 137.3 (d, $^2J_{C\text{-}F}$ = 7.7 Hz), 134.4 (d, $^3J_{C\text{-}F}$ = 9.6 Hz), 131.0 (d, $^4J_{C\text{-}F}$ = 4.0 Hz), 125.7, 118.8 (d, $^2J_{C\text{-}F}$ = 21.5 Hz), 86.1, 78.2, 52.4, 51.4, 41.5l, 40.2, 39.6, 38.3, 35.6, 28.7, 27.2, 26.4, 25.6, 24.9, 24.1, 23.0, 22.8, 22.6, 22.3. ^{11}B NMR (160 MHz, Chloroform-*d*) δ 29.6. ^{19}F NMR (564 MHz, Chloroform-*d*) δ -112.5. HRMS (DART-TOF$^+$): *m/z* for $C_{28}H_{42}BFN_3O_6$: calcd 546.3150, observed 546.3157 [M+H].

(-)-Pinanediol ((*S*)-1-((*R*)-2-(2-chloro-4-methoxybenzamido)-4-methylpentanamido)-3-methylbutyl)boronate (7d). White solid; yield = 251 mg, 45% (>95:5 dr); R_f = 0.30 (30% EtOAc in hexanes). ^{1}H NMR (400 MHz, Chloroform-*d*) δ 7.62 (d, J = 8.7 Hz, 1H), 6.89 (d, J = 2.5 Hz, 1H), 6.83 (dd, J = 8.7, 2.5 Hz, 1H), 6.75 (d, J = 8.3 Hz, 1H), 6.55 (brd, J = 5.1 Hz, 1H), 4.69 (td, J = 8.4, 5.9 Hz, 1H), 4.28 (dd, J = 8.8, 2.2 Hz, 1H), 3.81 (s, 3H), 3.21 (dt, J = 9.0, 5.9 Hz, 1H), 2.31 (ddt, J = 13.9, 8.9, 2.4 Hz, 1H), 2.15 (dtd, J = 10.7, 6.0, 2.1 Hz, 1H), 1.99 (t, J = 5.5 Hz, 1H), 1.89 (dq, J = 5.8, 3.0 Hz, 1H),

1.83 (ddd, *J* = 14.2, 3.2, 2.0 Hz, 1H), 1.80 – 1.70 (m, 2H), 1.69 – 1.58 (m, 2H), 1.46 (dt, *J* = 7.9, 6.3 Hz, 2H), 1.37 (s, 3H), 1.27 (s, 3H), 0.96 (d, *J* = 6.5 Hz, 3H), 0.95 (d, *J* = 6.2 Hz, 3H), 0.89 (d, *J* = 3.7 Hz, 3H), 0.88 (d, *J* = 3.7 Hz, 3H), 0.83 (s, 3H). ^{13}C NMR (126 MHz, Chloroform-*d*) δ 172.4, 166.1, 161.7, 132.0, 132.0, 126.5, 115.6, 113.1, 85.6, 77.9, 55.8, 51.7, 51.6, 41.1, 40.3, 39.8, 38.3, 35.8, 28.8, 27.3, 26.4, 25.6, 24.9, 24.2, 23.2, 23.0, 22.4, 22.2. ^{11}B NMR (128 MHz, Chloroform-*d*) δ 28.7. HRMS (ESI, positive): *m/z* for $C_{29}H_{45}BClN_2O_5$: calcd 547.3141, observed 547.3143 [M+H].

General Procedure for the synthesis of enantiopure boronic acids (8). The enantiopure boronic acids were prepared using a modified procedure.[40] In a small vial equipped with a magnetic stir bar under nitrogen atmosphere, was added pinanediol boronate **7**, phenylboronic acid (1.0 eq.) and HCl (3.0 M, 10 eq.) in 1:1 hexanes:MeOH (0.05 M). The reaction was left to stir overnight at room temperature. The reaction was monitored by TLC and LC-MS. Upon completion, the hexanes layer was removed. The MeOH layer was washed with hexanes (x2) and then MeOH layer was collected. The solvent was removed *in vacuo*. The crude mixture was loaded onto Celite and purified by flash column chromatography* using DCM:MeOH (1% MeOH → 5% MeOH, increasing by 1% increments → 10% MeOH → 15% MeOH) to afford pure enantiopure boronic acid **8**. The pure compound was dissolved in MeCN:H_2O (1:1) and lyophilized to provide the enantiopure boronic acid **8** as a fluffy white solid.

*Note: The boronic acids are streak on silica gel and reverse-phase C18. In order to recover appreciable amounts of boronic acid using normal-phase column chromatography, it is necessary to flush with ~6-8 column volumes of 15% MeOH in DCM. It is also important to use a smaller diameter column (~1 cm for 100 mg of starting material) to prevent the product from eluting too dilute.

((*R*)-1-((*S*)-2-(2-chloro-4-methoxybenzamido)-4-methylpentanamido)-3-methylbutyl)boronic acid (8a).

White solid; yield = 24 mg, 82%; Purity : >95% (as determined by ^{1}H NMR); R_f = 0.32 (9:1, DCM:MeOH). ^{1}H NMR (400 MHz, Methanol-d_4) δ 7.42 (d, *J* = 8.6 Hz, 1H), 7.03 (d, *J* = 2.4 Hz, 1H),

6.94 (dd, *J* = 8.6, 2.5 Hz, 1H), 4.79 (dd, *J* = 9.5, 5.6 Hz, 1H), 3.84 (s, 3H), 2.76 (dd, *J* = 8.6, 6.6 Hz, 1H), 1.87 – 1.76 (m, 2H), 1.74 – 1.59 (m, 2H), 1.35 (ddd, *J* = 7.9, 6.2, 3.3 Hz, 1H), 1.02 (d, *J* = 6. Hz, 3H), 1.00 (d, *J* = 6.4 Hz, 3H), 0.95 (s, 3H), 0.93 (s, 3H).^{13}C NMR (126 MHz, Methanol-d_4) δ 178.8, 169.9, 163.0, 133.3, 131.4, 128.7, 116.5, 113.8, 56.3, 50.0, 41.3, 41.1, 27.1, 25.9, 23.8, 23.1, 22.3, 21.9. ^{11}B NMR* (128 MHz, Methanol-d_4) δ 18.5 (tricoordinate boron), 13.2 (tetracoordinate boron). HRMS (ESI, positive): *m/z* for $C_{19}H_{29}BClN_2O_4$: calcd 394.1938, observed 394.1938 [M+H-H_2O].

*Note: Two signals arise in the ^{11}B NMR because there is some coordination from the amide oxygen to the boron center.[42,43]

((*R*)-1-((*S*)-2-([1,1'-biphenyl]-2-carboxamido)-4-methylpentanamido)-3-methylbutyl)boronic acid (8b). White solid; yield = 36 mg, 78%; Purity : >95% (as determined by ^{1}H NMR); R_f = 0.38 (9:1, DCM:MeOH). ^{1}H NMR (400 MHz, Methanol-d_4) δ 7.55 – 7.40 (m, 9H), 4.52 (dd, *J* = 10.3, 5.2 Hz, 1H), 2.72 (t, *J* = 7.6 Hz, 1H), 1.71 – 1.59 (m, 1H), 1.51 (ddd, *J* = 13.6, 10.3, 5.1 Hz, 1H), 1.40 – 1.30 (m, 3H), 1.21 – 1.07 (m, 1H), 0.93 (d, *J* = 6.6 Hz, 3H), 0.92 (d, *J* = 6.5 Hz, 3H), 0.82 (d, *J* = 6.6 Hz, 3H), 0.78 (d, *J* = 6.5 Hz, 3H). ^{13}C NMR (126 MHz, Methanol-d_4) δ 178.9, 173.1, 141.8, 141.4, 136.9, 131.3, 131.2, 129.7 (2C), 129.5 (2C), 128.9, 128.6, 128.3, 49.7, 41.1, 41.0, 27.0, 25.3, 23.8, 23.2, 22.4, 21.9. ^{11}B NMR (128 MHz, Methanol-d_4) δ 13.0. HRMS (ESI, positive): *m/z* for $C_{24}H_{32}BN_2O_3$: calcd 406.2538, observed 406.2538 [M+H-H_2O].

((*R*)-1-((*S*)-2-(4-fluoro-3-nitrobenzamido)-4-methylpentanamido)-3-methylbutyl)boronic acid (8c). Yellow solid; yield = 43 mg, 93%; Purity : >95% (as determined by ^{1}H NMR); R_f = 0.32 (9:1, DCM:MeOH). ^{1}H NMR (400 MHz, Methanol-d_4) δ 8.65 (dd, *J* = 7.1, 2.3 Hz, 1H), 8.25 (ddd, *J* = 8.7, 4.2, 2.3 Hz, 1H), 7.56 (dd, *J* = 10.7, 8.7 Hz, 1H), 4.83 (hidden, 1H), 2.75 (t, *J* = 7.6 Hz, 1H), 1.92 – 1.86 (m, 1H), 1.82 – 1.62 (m, 3H), 1.35 (t, *J* = 7.3 Hz, 2H), 1.02 (d, *J* = 6.3 Hz, 3H), 0.99 (d, *J* = 6.1 Hz, 3H), 0.93 (s, 3H), 0.92 (s, 3H). ^{13}C NMR (126 MHz, Methanol-d_4) δ 178.9, 166.9, 158.5 (d, $^1J_{C\text{-}F}$ = 267.8 Hz), 138.5 (d, $^2J_{C\text{-}F}$ = 8.6 Hz), 136.1 (d, $^3J_{C\text{-}F}$ = 9.8 Hz), 131.8 (d, $^4J_{C\text{-}F}$ = 4.0 Hz), 126.8 (d, $^3J_{C\text{-}F}$ = 2.0 Hz),

119.8 (d, $^{2}J_{C\text{-}F}$ = 21.6 Hz), 50.3, 41.0, 41.0, 27.0, 26.0, 23.7, 23.0, 22.5, 21.9. ^{11}B NMR (128 MHz, Methanol-d_4) δ 13.0. ^{19}F NMR (377 MHz, Methanol-d_4) δ -115.6. HRMS (DART-TOF$^+$): *m/z* for $C_{18}H_{26}BFN_3O_5$: calcd 394.1949, observed 394.1950 [M+H-H_2O].

((*S*)-1-((*R*)-2-(2-chloro-4-methoxybenzamido)-4-methylpentanamido)-3-methylbutyl)boronic acid (8d).

White solid; yield = 53 mg, 70%; Purity : >95% (as determined by ^{1}H NMR); R_f = 0.37 (9:1, DCM:MeOH). ^{1}H NMR (400 MHz, Methanol-d_4) δ 7.43 (d, *J* = 8.6 Hz, 1H), 7.03 (d, *J* = 2.5 Hz, 1H), 6.95 (dd, *J* = 8.6, 2.5 Hz, 1H), 4.79 (dd, *J* = 9.5, 5.6 Hz, 1H), 3.84 (s, 3H), 2.76 (dd, *J* = 8.6, 6.6 Hz, 1H), 1.87 – 1.76 (m, 2H), 1.74 – 1.57 (m, 2H), 1.35 (ddd, *J* = 7.9, 6.2, 3.6 Hz, 2H), 1.01 (d, *J* = 6.3 Hz, 3H), 1.00 (d, *J* = 6.3 Hz, 3H), 0.94 (s, 3H), 0.93 (s, 3H). ^{13}C NMR (126 MHz, Methanol-d_4) δ 178.9, 169.9, 163.0, 133.3, 131.4, 128.7, 116.5, 113.8, 56.3, 50.0, 41.3, 41.1, 27.1, 25.9, 23.8, 23.1, 22.3, 21.9. ^{11}B NMR* (128 MHz, Methanol-d_4) δ 13.2. HRMS (ESI, positive): *m/z* for $C_{19}H_{29}BClN_2O_4$: calcd 394.1940, observed 394.1947 [M+H-H_2O].

*Note: Two signals arise in the ^{11}B NMR because there is some coordination from the amide oxygen to the boron center.[42,43]

Computational modeling.

Protein preparation. The model of hClpP was based on the apo x-ray structure with PDB code 1TG6.[25] The crystal structure contains seven protein chains arranged as ring, corresponding to one half of the hClpP heptadecamer. The docking was performed in the active site of chain A, however chain B and G were also included in the model, since residues from both chain B and G are in the vicinity of the active site of chain A. The Protein preparation wizard in the Schrödinger Suite[44] was used for the following steps. Hydrogens were added and bond order were assigned. Co-crystallized water molecules as well as small organic molecules were removed. Protonation states were assigned using PropKa at pH 7.[45,46] The model was then relaxed through a restrained minimization with a maximum RMSD = 0.3 Å for heavy

atoms using the OLPS3 force field. As mentioned, the x-ray structure represents the apo state of hClpP. Therefore, minor adjustments were introduced to the structure prior to docking in order to mimic a substrate or ligand-bound state. The backbone of residues Gly68-Val70 and Pro124-Ser125 were slightly shifted to allow for hydrogen bonds to the amide bonds found in both the natural peptide substrates and the ligands in the virtual library studied here. In addition, the side chains of Val70, Met60 and His122 were also adjusted to allow access to the S1 pocket, which was otherwise restricted. In accordance with the non-covalent docking protocol described in this manuscript, the reactive residue, Ser97, was mutated to glycine prior to docking.

Library enumeration. The virtual compound library was constructed based on the isocyanide Ugi reaction. The starting materials that were available in-house were used for the enumeration, and consisted of 201 carboxylic acids, 79 aldehydes and 8 boronic acid isocyanides. The enumeration was performed in BIOVIA Pipeline Pilot,[34] and yielded 127,032 unique compounds. A set of filters was applied to remove molecules containing reactive functional groups as well as molecules with undesirable physiochemical properties, which reduced the number of compounds to 85,063. Finally, a hydrogen was added to the boron atom in each compound to obtain a tetrahedral geometry around the boron.

Docking. The compounds were prepared for docking using the LigPrep program[47] in the Schrödinger Suite. Protonation states were generated at pH = 7 ± 1 using Epik. The compounds were docked flexibly in the active site of the hClpP model utilizing the Glide docking program[35,48–50] which is part of the Schrödinger Suite.[47] The docking was performed in three stages (HTSV, SP, XP) using the Virtual Screening Workflow. The dimensions of the inner and outer box were set to 10 x 10 x 10 $Å^3$ and 30 x 30 x 30 $Å^3$, with the box centered at the center of the ligand used for creating the ligand-bound hClpP model. The hydroxyl groups of S125 and Y153 were treated as rotatable during the docking calculations. In all three docking stages, a maximum 5 Å distance constraint between C_α of G97 and boron was applied. Post-docking minimization was performed at all three stages. Top 10% was kept from the

HTSV and SP stage, respectively, and the top 2,500 compounds from the XP stage were kept for analysis. A single pose was saved per compound.

Biological Experiments.

Purification of Human ClpP and Human ClpX. Purification of untagged hClpP and His_6-ClpX was done according to Wong, K. S. *et al.*,[38] Leung, E. *et al.*[41] and Cole, A. *et al*.[20] with some slight modifications. *E. coli* SG1146, which is BL21(DE3) Δ*clpP*::*cat*[51] were transformed with pETSUMO2-CLPP(-MTS) and grown in Luria broth (LB) supplemented with+ 50 μg/mL kanamycin at 37 °C until OD600 reaches ~0.6. Protein expression was then induced with 1.0 mM isopropyl b-D-1-thiogalactopyranoside (IPTG) (Thermo-Fisher Scientific) for 3-4 hours. Cells were harvested by centrifugation, and then re-suspended in 25 mM TrisHCl, pH 7.5, 0.5 M NaCl, 10% glycerol, and 10 mM imidazole. Cells were then lysed by sonication, and the cell debris was removed by centrifugation. The SUMO-tagged hClpP was purified on Ni-NTA beads (Thermo-Fisher Scientific) using standard protocols. Subsequently, SUMO[52] protease was added to remove the *N*-terminal 2x(His6-thrombin)-SUMO tag. The purified untagged hClpP was concentrated with an Amicon Ultra-50 centrifugal filter unit (10000 MWCO) (EMD Millipore) at 4 °C. A similar protocol was used for hClpX with the following difference. Plasmid pProEX htb ClpX encoding human His_6-TEV-ClpX was transformed into B21 Gold DE3. Then bacteria were plated on LB-agar plates containing 50 μg/ml ampicillin and incubated overnight at 37 °C. The following day, individual colonies were grown overnight at 37 °C in LB medium containing 50 μg/ml ampicillin. His_6-hClpX expression was induced with 1.0 mM IPTG in Luria broth containing 50 μg/ml ampicillin. Bacteria were collected after 4 h, and the pellet was frozen at −70C. After sonication, His_6-ClpX protein was purified on Ni-agarose and was dialyzed for 2 h at 4 °C in dialysis buffer (50 mM Tris-HCl [pH 7.5], 200 mM KCl, 25mM $MgCl_2$, 10% g1ycerol, 1 mM DTT, and 0.1 mM EDTA). Both recombinant proteins were stored at -70 °C. All fractions collected during the purification were analyzed by SDS-PAGE.

WLA-AMC assay. ClpP peptidase activity was measured according to Wong, K. S. *et al*.[38] with some modifications. 3.6 μM ClpP (monomer concentration) was dissolved in assay buffer (50 mM Tris-Cl pH 8.0, 100 mM KCl, 10 mM $MgCl_2$, 5% glycerol and 0.02% Triton X-100 and 1 mM DTT). Tested compounds were added to the hClpP solution and incubated for 60 min at 37 °C. The reaction was initiated with 0.3 mM *N*-acetyl-Trp-Leu-Ala-AMC (R&D, Ac-WLA-AMC) (final substrate concentration 48 μM) and read for releasing fluorescence at 20 sec intervals for 1 h at 350/460 nm at 37 °C. The rate of ClpP activity was determined by calculating the slope (in the linear range) and presented as percentage of a DMSO control. A serial dilution of compound **1** was made with a starting concentration of 140 μM and a final concentration of 1.09 μM after 7 dilutions. Serial dilutions of compounds **4a**-**4e** and **8a**-**8c** were made with a starting concentration of 140 μM and a final concentration of 0.1 μM after 9 dilutions. A serial dilution of compound **4f** was made with a starting concentration of 100 μM and a final concentration of 0.1 μM after 8 dilutions.

FITC-casein assay. The protease activity of hClpXP was assessed based on the described method by Leung, E. *et al*.[41] Human recombinant ClpP (1.0 μM) and ClpX (3.0 μM) were incubated in assay buffer consisting of 25 mM *N*-2-hydroxyethylpiperazine-*N*'-2-ethanesulfonic acid (HEPES) (pH 7.4), 5 mM $MgCl_2$, 5 mM KCl, 0.03% Tween 20, and 10% glycerol with an ATP regeneration system of 16 mM creatine phosphate and 13 U/ml creatine kinase supplemented with 3 mM ATP for 10 min at 37 °C. Thereafter, tested compounds were added to the hClpXP solution and incubated for 60 min at 37 °C. The reaction was initiated with 0.1 mM casein-fluorescein isothiocyanate (Sigma, FITC-casein, final concentration 4.6 μM) and read for releasing fluorescence at 20 sec intervals for 1 h at 485/535 nm at 37 °C. The rate of ClpXP activity was determined by calculating the slope (in the linear range) and presented as percentage of a DMSO control. Serial dilutions of compounds **4a**-**4c** were made with a starting concentration of 28 μM and a final concentration of 0.22 μM after 7 dilutions. Serial dilutions of compounds **8a** and **8c** were made with a starting concentration of 28 μM and a final concentration of

0.55 μM after 9 dilutions. A serial dilution of compound **8b** was made with a starting concentration of 14 μM and a final concentration of 0.05 μM after 8 dilutions.

IC_{50} Calculation. GraphPad Prizm Software was used to determine the IC_{50} by fitting dose-response curves. Peptidase and protease activity of compound-treated hClpP were normalized to DMSO-treated controls. The concentrations of the compounds were transformed into their logarithm. The data were analyzed by non-linear regression and then the equation "log(inhibitor) vs. response -- Variable slope" was chosen. The fitting method used was the least squares method. The goal was to determine the IC_{50} of the inhibitor - the concentration that provokes hClpP activity half-way between the maximal response and the maximally inhibited response. In the case of compound **4f** which did not inhibit hClpP completely, the absolute IC_{50} was calculated by constraining the bottom of the curve to be equal to 0.

Supporting Information

The Supporting Information is available free of charge on the ACS Publications website.

Molecular formula strings and biological data.

HPLC traces for *N*-Ac-Phe-Ala-Pro-His-B(MIDA) and compounds 1 and 7a-d. Description of the substrate tolerance of the U4CR with boryl isocyanides and attempted synthesis of 8e. Description of the OICR In-house filters. Reduced virtual library of hClpP inhibitors, molecules selected for synthesis and sequence homology comparison. Crystal structure determination. Dose-response curves for WLA-AMC and FITC-casein assays. NMR traces of characterized compounds.

Frequency analysis.

Acession Codes

Atomic coordinates and structure factors of ***anti*-4a** bound to SaClpP have been deposited to the Protein Data Bank (PDB) under accession number 6HM0. Authors will release the atomic coordinates and experimental data upon article publication.

Corresponding Author

*Email: ayudin@chem.utoronto.ca

ORCID

Andrei K. Yudin: 0000-0003-3170-9103

Joanne Tan: 0000-0001-6676-1468

Diego B. Diaz: 0000-0001-8293-1084

Author Contributions

J.T., D.B.D., W.S. and A.F.B. carried out all of the synthetic work and characterizations. J.J.G. developed the virtual library and screening protocol, and performed the virtual filtering. Y.J. ran all of the biological assays. E.C.G. obtained and solved the crystal structures. G.P. provided guidance and advice in regards to virtual design and screen. A.D.S. provided guidance and advice regarding the biological assays. R.L. provided guidance and advice towards the crystallography. A.K.Y. conceived the initial idea and provided guidance and advice for the chemistry. All authors contributed to the preparation and revision of the manuscript.

Acknowledgements

J.T. would like to thank NSERC CGS-D and OGS for funding. D.B.D. would like to thank NSERC PGS-D for funding. We would also like to thank Dr. Alessandro Dhatti from Mount Sinai for running the preliminary hClpP screens and Dr. Kong Nyugen, who is currently at Atomwise, San Francisco, CA, USA for performing the initial enumeration and docking of the previous virtual library. This work was supported by the Leukemia and Lymphoma Society, Natural Science and Engineering Research Council, Canadian Institutes of Health Research, the Ontario Institute for Cancer Research with funding provided by the Ontario Ministry of Research and Innovation, the Princess Margaret Cancer Centre Foundation, and the Ministry of Long Term Health and Planning in the Province of Ontario, and ALSAC St. Jude Children's Research Hospital. Crystallographic support was provided by the St. Jude X-ray Center. Data were

collected at Southeast Regional Collaborative Access Team (SER-CAT) 22-BM beamline at the Advanced Photon Source, Argonne National Laboratory. SER-CAT is supported by its member institutions (see www.ser-cat.org/members.html), and equipment grants (S10_RR25528 and S10_RR028976) from the National Institutes of Health. Use of the Advanced Photon Source was supported by the U. S. Department of Energy, Office of Science, Office of Basic Energy Sciences, under Contract No. W-31-109-Eng-38. A.D.S holds the Barbara Baker Chair in Leukemia and Related Diseases.

Abbreviations Used.

BCM, boron-containing molecules; ABHD3, α/β-hydrolyase domain 3; MIDA, *N*-methyliminodiacetic acid; ClpP, caseinolytic protease P; ClpA, caseinolytic protease A; ClpC, caseinolytic protease C; ClpX, caseinolytic protease X; hClpP, human caseinolytic protease P; hClpX, human caseinolytic protease X; hClpXP, human caseinolytic protease XP complex; AML, acute myeloid leukemia; *Ec*ClpX, *Escherichia coli* caseinolytic protease X; FITC-casein, fluorescein-isothiocyanate-labelled casein; GFP, green fluorescent protein; *Mt*ClpP, *Mycobacterium tuberculosis* caseinolytic protease P; WLA-AMC, Ac-Trp-Leu-Ala-7-amino-4-methylcoumarin; U4CR, Ugi 4-component reaction; SCAR, Steric-Clashes Alleviating Receptor; HTS, High-throughput screening; TFE, trifluoroethanol; *Sa*ClpP, *Staphylococcus aureus* caseinolytic protease P; DIPEA, *N*,*N*-diisopropylethylamine; HFIP, hexafluoroisopropanol; HCl, hydrochloric acid; ITPG, isopropyl b-D-1-thiogalactopyranoside; HEPES, *N*-2-hydroxyethylpiperazine-*N*'-2-ethanesulfonic acid

References

(1) Adamczyk-Woźniak, A.; Borys, K. M.; Sporzyński, A. Recent Developments in the Chemistry and Biological Applications of Benzoxaboroles. *Chem. Rev.* **2015**, *115*, 5224–5247.

(2) Baker, S. J.; Ding, C. Z.; Akama, T.; Zhang, Y.-K.; Hernandez, V.; Xia, Y. Therapeutic Potential of Boron-Containing Compounds. *Future Med. Chem.* **2009**, *1*, 1275–1288.

(3) Baker, S. J.; Tomsho, J. W.; Benkovic, S. J. Boron-Containing Inhibitors of Synthetases. *Chem. Soc. Rev.* **2011**, *40*, 4279–4285.

(4) Hall, D. G. *Boronic Acids: Preparation and Applications in Organic Synthesis Medicine and Materials*, 2nd ed.; Wiley-VCH: Weinheim, 2011.

(5) Smoum, R.; Rubinstein, A.; Dembitsky, V. M.; Srebnik, M. Boron Containing Compounds as Protease Inhibitors. *Chem. Rev.* **2012**, *112*, 4156–4220.

(6) Touchet, S.; Carreaux, F.; Carboni, B.; Bouillon, A.; Boucher, J.-L. Aminoboronic Acids and Esters: From Synthetic Challenges to the Discovery of Unique Classes of Enzyme Inhibitors. *Chem. Soc. Rev.* **2011**, *40*, 3895–3914.

(7) Das, B. C.; Thapa, P.; Karki, R.; Schinke, C.; Das, S.; Kambhampati, S.; Banerjee, S. K.; Van Veldhuizen, P.; Verma, A.; Weiss, L. M.; Evans, T. Boron Chemicals in Diagnosis and Therapeutics. *Future Med. Chem.* **2013**, *5*, 653–676.

(8) Bross, P. F.; Kane, R.; Farrell, A. T.; Abraham, S.; Benson, K.; Brower, M. E.; Bradley, S.; Gobburu, J. V.; Goheer, A.; Lee, S.-L.; Leighton, J.; Liang, C. Y.; Lostritto, R. T.; McGuinn, W. D.; Morse, D. E.; Rahman, A.; Rosario, L. A. Verbois, S. L.; Williams, G.; Wang, Y.-C.; Pazdur, R. Approval Summary for Bortezomib for Injection in the Treatment of Multiple Myeloma. *Clin. Cancer Res.* **2004**, *10*, 3954–3964.

(9) Diaz, D. B.; Yudin, A. K. The Versatility of Boron in Biological Target Engagement. *Nat. Chem.* **2017**, *9*, 731–742.

(10) Dean, J. A. *Lange's Handbook of Chemistry*, Thirteenth.; McGraw-Hill: New York, 1985.

(11) Spencer, J.; Burd, A. P.; Goodwin, C. A.; Mérette, S. A. M.; Scully, M. F.; Adatia, T.; Deadman, J. J. Synthesis of *Ortho*-Modified Mercapto- and Piperazino-Methyl-Phenylboronic Acid Derivatives. *Tetrahedron* **2002**, *58*, 1551–1556.

(12) Laplante, C.; Hall, D. G. Direct Mono-*N*-Methylation of Solid-Supported Amino Acids: A Useful Application of the Matteson Rearrangement of α-Aminoalkylboronic Esters. *Org. Lett.* **2001**, *3*, 1487–1490.

(13) Matteson, D. S.; Sadhu, K. M. Synthesis of 1-Amino-2-Phenylethane-1-Boronic Acid Derivatives. *Organometallics* **1984**, *3*, 614–618.

(14) He, Z.; Yudin, A. K. Amphoteric α-Boryl Aldehydes. *J. Am. Chem. Soc.* **2011**, *133*, 13770–13773.

(15) St. Denis, J. D.; Zajdlik, A.; Tan, J.; Trinchera, P.; Lee, C. F.; He, Z.; Adachi, S.; Yudin, A. K. Boron-Containing Enamine and Enamide Linchpins in the Synthesis of Nitrogen Heterocycles. *J. Am. Chem. Soc.* **2014**, *136*, 17669–17673.

(16) Diaz, D. B.; Scully, C. C. G.; Liew, S. K.; Adachi, S.; Trinchera, P.; St. Denis, J. D.; Yudin, A. K. Synthesis of Aminoboronic Acid Derivatives from Amines and Amphoteric Boryl Carbonyl Compounds. *Angew. Chem. Int. Ed.* **2016**, *55*, 12659–12663.

(17) Zajdlik, A.; Wang, Z.; Hickey, J. L.; Aman, A.; Schimmer, A. D.; Yudin, A. K. α-Boryl Isocyanides Enable Facile Preparation of Bioactive Boropeptides. *Angew. Chem. Int. Ed.* **2013**, *52*, 8411–8415.

(18) Tan, J.; Iii Cognetta, A. B.; Diaz, D. B.; Lum, K. M.; Adachi, S.; Kundu, S.; Cravatt, B. F.; Yudin, A. K. Multicomponent Mapping of Boron Chemotypes Furnishes Selective Enzyme Inhibitors. *Nat. Commun.* **2017**, *8*, 1760.

(19) Ye, F.; Li, J.; Yang, C.-G. The Development of Small-Molecule Modulators for ClpP Protease Activity. *Mol. BioSyst.* **2017**, *13*, 23–31.

(20) Cole, A.; Wang, Z.; Coyaud, E.; Voisin, V.; Gronda, M.; Jitkova, Y.; Mattson, R.; Hurren, R.; Babovic, S.; Maclean, N.; Restall, I.; Wang, X.; Jeyaraju, D. V.; Sukhai, M. A.; Prabha, S.; Bashir, S.; Ramakrishnan, A.; Leung, E.; Qia, Y. H.; Zhang, N.; Combes, K. R.; Ketela, T.; Lin, F.; Houry, W. A.; Aman, A.; Al-awar, R.; Zheng, W.; W., Erno; X., Chang J.; Dick, J.; Wang, J. C. Y.; Moffat, J.; Minden, M. D.; Eaves, C. J.; Bader, G. D.; Hao, Z.; Kornblau, S. M.; Raught, B.; Schimmer, A. D. Inhibition of the Mitochondrial Protease ClpP as a Therapeutic Strategy for Human Acute Myeloid Leukemia. *Cancer Cell* **2015**, *27*, 864–876.

(21) Bhandari, V.; Wong, K. S.; Zhou, J. L.; Mabanglo, M. F.; Batey, R. A.; Houry, W. A. The Role of ClpP Protease in Bacterial Pathogenesis and Human Diseases. *ACS Chem. Biol.* **2018**, *13*, 1413–1425.

(22) Hackl, M. W.; Lakemeyer, M.; Dahmen, M.; Glaser, M.; Pahl, A.; Lorenz-Baath, K.; Menzel, T.; Sievers, S.; Böttcher, T.; Antes, I.; Waldmann, H.; Sieber, S. A. Phenyl Esters Are Potent Inhibitors of Caseinolytic Protease P and Reveal a Stereogenic Switch for Deoligomerization. *J. Am. Chem. Soc.* **2015**, *137*, 8475–8483.

(23) Gronauer, T. F.; Mandl, M. M.; Lakemeyer, M.; Hackl, M. W.; Meßner, M.; Korotkov, V. S.; Pachmayr, J.; Sieber, S. A. Design and Synthesis of Tailored Human Caseinolytic Protease P Inhibitors. *Chem. Commun.* **2018**, *54*, 9833–9836.

(24) Kang, S. G.; Ortega, J.; Singh, S. K.; Wang, N.; Huang, N. N.; Steven, A. C.; Maurizi, M. R. Functional Proteolytic Complexes of the Human Mitochondrial ATP-Dependent Protease, hClpXP. *J. Biol. Chem.* **2002**, *277*, 21095–21102.

(25) Kang, S. G.; Maurizi, M. R.; Thompson, M.; Mueser, T.; Ahvazi, B. Crystallography and Mutagenesis Point to an Essential Role for the *N*-Terminus of Human Mitochondrial ClpP. *J. Struct. Biol.* **2004**, *148*, 338–352.

(26) In reference 22 only compounds with an IC_{50} value lower than 2 μM were considered inhibitors.

The following reference described a molecule that weakly binds to hClpXP with an IC_{50} value of 29 μM: Knott, K.; Fishovitz, J.; Thorpe, S. B.; Lee, I.; Santos, W. L. *N*-Terminal Peptidic Boronic Acids Selectively Inhibit Human ClpXP. *Org. Biomol. Chem.* **2010**, *8*, 3451–3456.

(27) Zhu, K.; Borrelli, K. W.; Greenwood, J. R.; Day, T.; Abel, R.; Farid, R. S.; Harder, E. Docking Covalent Inhibitors: A Parameter Free Approach to Pose Prediction and Scoring. *J. Chem. Inf. Model.* **2014**, *54*, 1932–1940.

(28) London, N.; Miller, R. M.; Krishnan, S.; Uchida, K.; Irwin, J. J.; Eidam, O.; Gibold, L.; Cimermančič, P.; Bonnet, R.; Shoichet, B. K.; Taunton, J. Covalent Docking of Large Libraries for the Discovery of Chemical Probes. *Nat. Chem. Biol.* **2014**, *10*, 1066–1072.

(29) Bianco, G.; Forli, S.; Goodsell, D. S.; Olson, A. J. Covalent Docking Using Autodock: Two-Point Attractor and Flexible Side Chain Methods. *Protein Sci.* **2016**, *25*, 295–301.

(30) Ouyang, X.; Zhou, S.; Su, C. T. T.; Ge, Z.; Li, R.; Kwoh, C. K. CovalentDock: Automated Covalent Docking with Parameterized Covalent Linkage Energy Estimation and Molecular Geometry Constraints. *J. Comput. Chem.* **2013**, *34*, 326–336.

(31) Moreira, W.; Ngan, G. J. Y.; Low, J. L.; Poulsen, A.; Chia, B. C. S.; Ang, M. J. Y.; Yap, A.; Fulwood, J.; Lakshmanan, U.; Lim, J.; Khoo, A. Y. T.; Flotow, H.; Hill, J.; Raju, R. M.; Rubin, E. J.; Dick, T. Target Mechanism-Based Whole-Cell Screening Identifies Bortezomib as an Inhibitor of Caseinolytic Protease P in Mycobacteria. *MBio* **2015**, *6*, e00253-15.

(32) Akopian, T.; Kandror, O.; Tsu, C.; Lai, J. H.; Wu, W.; Liu, Y.; Zhao, P.; Park, A.; Wolf, L.; Dick, L. R.; Rubin, E. J.; Bachovchin, W.; Goldberg, A. L. Cleavage Specificity of *Mycobacterium Tuberculosis* ClpP1P2 Protease and Identification of Novel Peptide Substrates and Boronate Inhibitors with Anti-Bacterial Activity. *J. Biol. Chem.* **2015**, *290*, 11008–11020.

(33) He, Z.; Zajdlik, A.; St. Denis, J. D.; Assem, N.; Yudin, A. K. Boroalkyl Group Migration Provides a Versatile Entry into α-Aminoboronic Acid Derivatives. *J. Am. Chem. Soc.* **2012**, *134*, 9926–

9929.

(34) Dassault Systèmes BIOVIA, BIOVIA Pipeline Pilot, Release 2017, San Diego: Dassault Systèmes, [2017].

(35) **Schrödinger Release 2017-3**: Glide, Schrödinger, LLC, New York, NY, 2017.

(36) Ai, Y.; Yu, L.; Tan, X.; Chai, X.; Liu, S. Discovery of Covalent Ligands via Noncovalent Docking by Dissecting Covalent Docking Based on a "Steric-Clashes Alleviating Receptor (SCAR)" Strategy. *J. Chem. Inf. Model.* **2016**, *56*, 1563–1575.

(37) Gersch, M.; Stahl, M.; Poreba, M.; Dahmen, M.; Dziedzic, A.; Drag, M.; Sieber, S. A. Barrel-Shaped ClpP Proteases Display Attenuated Cleavage Specificities. *ACS Chem. Biol.* **2016**, *11*, 389–399.

(38) Wong, K. S.; Mabanglo, M. F.; Seraphim, T. V.; Molica, A.; Mao, Y.-Q.; Rizzolo, K.; Leung, E.; Moutaoufik, M. T.; Hoell, L.; Phanse, S.; Goodreid, J.; Barbosa, L. R. S.; Ramos, C. H. I.; Babu, M.; Mennella, V.; Batey, R. A.; Schimmer, A. D.; Houry, W. A. Acyldepsipeptide Analogs Dysregulate Human Mitochondrial ClpP Protease Activity and Cause Apoptotic Cell Death. *Cell Chem. Biol.* **2018**, *25*, P1017-1030.E9.

(39) Tsai, D. J. S.; Jesthi, P. K.; Matteson, D. S. Diastereoselection in Reactions of Pinanediol Dichloromethaneboronate. *Organometallics* **1983**, *2*, 1543–1545.

(40) Pickersgill, I. F.; Bishop, J.; Ammoscato, V.; Munk, S.; Lo, Y.; Chiu, F.-T.; Kulkarni, V. R. Synthesis of Bortezomib. EP 2377869 A1, 2011.

(41) Leung, E.; Datti, A.; Cossette, M.; Goodreid, J.; McCaw, S. E.; Mah, M.; Nakhamchik, A.; Ogata, K.; El Bakkouri, M.; Cheng, Y. Q.; Wodak, S. J.; Eger, B. T.; Pai, E. F.; Liu, J.; Gray-Owen, S.; Batey, R. A.; Houry, W. A. Activators of Cylindrical Proteases as Antimicrobials: Identification and Development of Small Molecule Activators of ClpP Protease. *Chem. Biol.* **2011**, *18*, 1167–1178.

(42) López, A.; Clark, T. B.; Parra, A.; Tortosa, M. Copper-Catalyzed Enantioselective Synthesis of β-Boron β-Amino Esters. *Org. Lett.* **2017**, *19*, 6272–6275.

(43) Kaldas, S. J.; Rogova, T.; Nenajdenko, V. G.; Yudin, A. K. Modular Synthesis of β-Amino Boronate Peptidomimetics. *J. Org. Chem.* **2018**, *83*, 7296–7302.

(44) **Schrödinger Suite 2017-3**: Protein Preparation Wizard; Epik, Schrödinger, LLC, New York, NY, 2016; Impact, Schrödinger, LLC, New York, NY, 2016; Prime, Schrödinger, LLC, New York, NY, 2017.

(45) Olsson, M. H. M.; Søndergaard, C. R.; Rostkowski, M.; Jensen, J. H. PROPKA3: Consistent Treatment of Internal and Surface Residues in Empirical pK_a Predictions. *J. Chem. Theory Comput.* **2011**, *7*, 525–537.

(46) Søndergaard, C. R.; Olsson, M. H. M.; Rostkowski, M.; Jensen, J. H. Improved Treatment of Ligands and Coupling Effects in Empirical Calculation and Rationalization of pK_a values. *J. Chem. Theory Comput.* **2011**, *7*, 2284–2295.

(47) **Schrödinger Release 2017-3**: LigPrep, Schrödinger, LLC, New York, NY, 2017.

(48) Friesner, R. A.; Banks, J. L.; Murphy, R. B.; Halgren, T. A.; Klicic, J. J.; Mainz, D. T.; Repasky, M. P.; Knoll, E. H.; Shelley, M.; Perry, J. K.; Shaw, D. E.; Francis, P.; Shenkin, P. S. Glide: A New Approach for Rapid, Accurate Docking and Scoring. 1. Method and Assessment of Docking Accuracy. *J. Med. Chem.* **2004**, *47*, 1739–1749.

(49) Friesner, R. A.; Murphy, R. B.; Repasky, M. P.; Frye, L. L.; Greenwood, J. R.; Halgren, T. A.; Sanschagrin, P. C.; Mainz, D. T. Extra Precision Glide: Docking and Scoring Incorporating a Model of Hydrophobic Enclosure for Protein-Ligand Complexes. *J. Med. Chem.* **2006**, *49*, 6177–6196.

(50) Halgren, T. A.; Murphy, R. B.; Friesner, R. A.; Beard, H. S.; Frye, L. L.; Pollard, W. T.; Banks, J. L. Glide: A New Approach for Rapid, Accurate Docking and Scoring. 2. Enrichment Factors in

Database Screening. *J. Med. Chem.* **2004**, *47*, 1750–1759.

(51) Kimber, M. S.; Yu, A. Y. H.; Borg, M.; Leung, E.; Chan, H. S.; Houry, W. A. Structural and Theoretical Studies Indicate That the Cylindrical Protease ClpP Samples Extended and Compact Conformations. *Structure* **2010**, *18*, 798–808.

(52) Lee, C.-D.; Sun, H.-C.; Hu, S.-M.; Chiu, C.-F.; Homhuan, A.; Liang, S.-M.; Leng, C.-H.; Wang, T.-F. An Improved SUMO Fusion Protein System for Effective Production of Native Proteins. *Protein Sci.* **2008**, *17*, 1241–1248.

Table of Contents Graphic

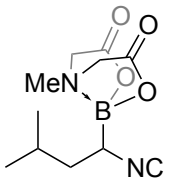

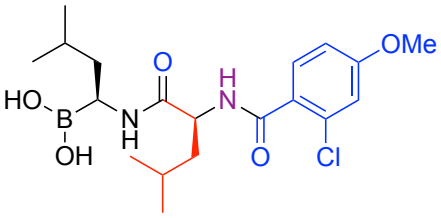

inactive

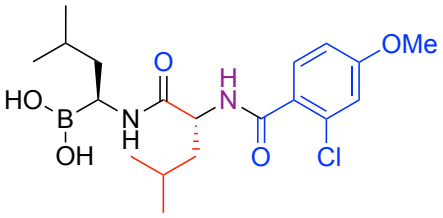

inactive

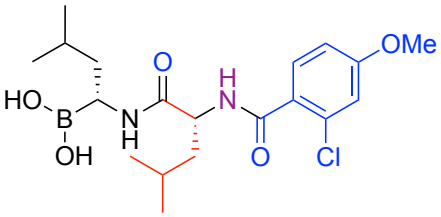

inactive

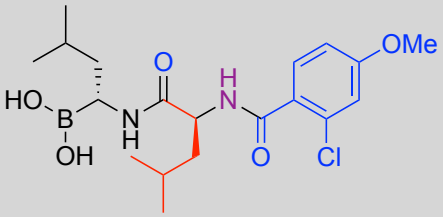

IC_{50} hClpXP = 0.8 μM